

Molecular mechanisms and brain morphology controlled by the transcription factor REST with relevance to Alzheimer's disease

Dzenana Becic

School of Pharmacy and Biomedical Science

A thesis submitted in partial fulfilment of the requirements for the degree of **MSc by Research** at the University of Central Lancashire (UCLan)

March, 2020

STUDENT DECLARATION FORM



Type of Award **Masters by Research**

School **Pharmacy and Biomedical Science**

1. Concurrent registration for two or more academic awards

I declare that while registered as a candidate for the research degree, I have not been a registered candidate or enrolled student for another award of the University or other academic or professional institution

2. Material submitted for another award

I declare that no material contained in the thesis has been used in any other submission for an academic award and is solely my own work

3. Collaboration

Where a candidate's research programme is part of a collaborative project, the thesis must indicate in addition clearly the candidate's individual contribution and the extent of the collaboration. Please state below:

4. Use of a Proof-reader

No proof-reading service was used in the compilation of this thesis.

Signature of Candidate _____

Print name: **Dzenana Becic**

Abstract

Alzheimer's disease (AD) is a major global health concern. Investigating the molecular mechanisms underlying AD will help develop new treatment strategies. The RE1-silencing transcription factor (REST) has been previously implicated in AD and is neuroprotective in the human brain, a function which was found to be lost in those diagnosed with AD. However, the molecular mechanisms underlying this are unclear. This study has employed a previously generated genetically modified conditional knockout (cKO) mouse model lacking REST in the brain, with inactivation only in the postnatal forebrain, in excitatory neurons (from 2-3 weeks of age). Wielding histological analysis, the different regions of the hippocampus CA1, CA2, CA3 and the dentate gyrus (DG) have been studied, analysing a possible neurodegenerative phenotype. Analysis of samples using western blot experiments and antibodies, against various proteins has allowed the investigation of the potential molecular mechanisms involved and aimed to correlate previously observed RNA changes in the brain of *Rest* cKO mice to their translated protein level. The findings of this study have allowed some tentative conclusions to be drawn which help with understanding the role of REST in the brain. This study has shown a possible neurodegenerative effect in the CA2 region of the hippocampus in *Rest* cKO mice using immunohistochemical (IHC) analysis. Furthermore, regarding a social memory related phenotype previously observed by the supervisor, a protein with a strong association to social memory impairment, Vasopressin V1B receptor (V1BR), was found to decrease in *Rest* cKO mice. Implying two possible conclusions regarding the CA2 region of the hippocampus; a possible neurodegenerative phenotype or an impairment in social memory. Another principal finding revealed by this study showed lower levels of phosphorylated CREB (Ser133) protein in *Rest* cKO mice. This important finding could suggest that a dysregulation in REST which leads to AD could occur due to a dysfunction in the mechanisms of CREB phosphorylation, associating memory loss to a lack of REST, a relationship which has not previously been made. The results from this study demonstrate the importance of research in REST and some features of neurodegeneration which should be further explored to allow potential therapeutic agents to be established.

Keywords: Alzheimer's disease, REST, Vasopressin V1B receptor, Phosphorylated CREB, CA2

Contents

	<i>Page</i>
List of figures and tables	6
Glossary and Abbreviations	7
1.0 Introduction	9
1.1 REST and Alzheimer's disease	9
1.2 Immediate early genes (IEGs) and their regulation in memory	11
1.3 Morphological characteristics in neurodegeneration	14
1.4 The CA2	16
1.5 The role of the CA2 in memory impairment	17
1.6 Protein involvement in memory impairment	18
1.7 A novel behavioural phenotype in <i>Rest</i> cKO mice	19
1.8 Experimental aims	20
2.0 Methods	20
2.1 <i>Rest</i> conditional knockout mice	20
2.2 Cryostat sectioning	20
2.3 Haematoxylin staining	21
2.4 Cresyl Violet (Nissl) staining	21
2.5 Immunohistochemistry	22
2.6 Citrate antigen retrieval	22
2.7 Protein lysate preparation	23
2.8 Nuclear extraction	24
2.9 Pierce BCA protein assay	25
2.10 SDS-PAGE gel electrophoresis	25
2.11 Activation of PVDF membrane	25
2.12 Wet transfer	25
2.13 Trans-blot turbo semi-dry transfer	26
2.14 Western blotting	26
2.15 Image acquisition	26
2.16 Quantification	27
2.17 Statistical analysis	27
2.18 Antibodies	28
3.0 Results	29
3.1 Nuclear extraction optimisation	29
3.2 Antibody optimisation	30
3.3 Testing the trans-blot turbo semi-dry transfer system	30
3.4 Testing PVDF membranes	30
3.5 Pilot analysis of <i>Rest</i> cKO and control in homogenate and nuclear extraction samples	32
3.6 ARC	33
3.7 HDAC2	35
3.8 CREB	37
3.9 Phosphorylated CREB (Ser133)	39
3.10 NPAS4	40
3.11 C-FOS	41
3.12 EGR-1	42

	<i>Page</i>
4.0 Immunohistochemical analysis	43
4.1 NeuN	43
4.2 GFAP	46
4.3 Synaptophysin	48
4.4 MAP2	49
5.0 Experiments on social memory related mechanisms	51
5.1 Vasopressin V1B receptor	51
5.2 Oxytocin receptor	52
5.3 Corticotrophin releasing factor	52
5.4 Identifying the CA2	53
6.0 Discussion	54
7.0 Concluding remarks	59
8.0 References	61
9.0 Appendix	68
Appendix A: Preparation of Reagents	68

Figures and tables

		<i>Page</i>
Figure 1	The regions of the hippocampus identified	16
Figure 2	Homogenisation and Nuclear Extraction method	24
Figure 3	Determination of the efficiency of different nuclear extraction protocols	29
Figure 4	Optimisation of antibodies, transfer system and PVDF membrane	31
Figure 5	An increase in ARC, NPAS4 and HDAC2 protein in <i>Rest</i> cKO in nuclear fractions but a decrease in CREB	32
Figure 6	Increase in ARC protein for <i>Rest</i> cKO mice in the cortical homogenate samples but a decrease in cortical nuclear fractions	34
Figure 7	An increase in HDAC2 protein in the cortex of <i>Rest</i> Cko	36
Figure 8	No difference in CREB protein expression between <i>Rest</i> cKO and controls in the cortex or hippocampus	38
Figure 9	A reduction in the levels of phosphorylated CREB protein observed in the <i>Rest</i> cKO samples	39
Figure 10	An increase in NPAS4 protein observed in control samples compared to <i>Rest</i> cKO	40
Figure 11	Multiple C-FOS protein bands observed in the homogenate and nuclear fractions	41
Figure 12	Multiple EGR-1 protein bands observed in the homogenate and nuclear fractions	42
Figure 13	The hippocampus with NeuN staining	43
Figure 14	A greater number of neuronal nuclei observed in the CA1 and DG region of the hippocampus in <i>REST</i> cKO	45
Figure 15	Astrocytes in <i>Rest</i> cKO and control samples in lateral sections of the hippocampus	46
Figure 16	An increase in astrocytes in <i>Rest</i> cKO in the CA1	47
Figure 17	Using synaptophysin as a marker of synapses proved too difficult for analysis	48
Figure 18	Using MAP2 as a marker of dendrites	49
Figure 19	An increase in V1BR protein in the <i>Rest</i> cKO samples in the cortex	51
Figure 20	Higher levels of oxytocin receptor protein in <i>Rest</i> cKO but lower levels of CRF	52
Figure 21	Identification of the CA2 on NeuN IHC sections	53
		<i>Page</i>
Table 1	Antibodies	28
Table 2	Table showing the properties analysed in dendrites in <i>Rest</i> cKO and controls	50

Abbreviations

AD	Alzheimer's Disease
A β	Amyloid β
ANOVA	Analysis of variance
BCA	Bicinchoninic acid
BSA	Bovine serum albumin
ChAT	Choline acetyltransferase
cKO	Conditional knockout
CNS	Central nervous system
CREB	cAMP response element-binding protein
CRF	Corticotrophin releasing factor
DAB	3,3'-diaminobenzidine
DG	Dentate Gyrus
DTT	Dithiothreitol
EC	Entorhinal Cortex
ECL	Enhanced chemiluminescence
EDTA	Ethylenediamine tetra-acetic acid
GFAP	Glial fibrillary acid protein
HDAC2	Histone deacetylase 2
IEG	Immediate early gene
IHC	Immunohistochemistry
MAP2	Microtubule associated protein 2
MCI	Mild cognitive impairment
MOPS	3-(N-morpholino) Propanesulfonic acid
NaCl	Sodium chloride
NFT	Neurofibrillary tangles
NMDA	N-methyl-D-aspartate
NRSE	Neuron-restrictive silencer element
OCT	Optimal cutting temperature
OXTR	Oxytocin receptor
PBS	Phosphate buffered saline
PNN	Perineuronal net
PVDF	Polyvinylidene fluoride

REST	Repressor element 1-silencing transcription factor
RIPA	Radioimmunoprecipitation assay
Rpm	Rotations per minute
SDS	Sodium dodecyl sulphate
V1BR	Vassopressin V1B receptor

1.0 Introduction

Alzheimer's disease (AD) is the most common type of dementia. The greatest risk factor for this neurodegenerative disease is age, followed by a dysregulation of AD related genes such as *ApoE4* (Safieh *et al.*, 2019). Identification of AD through pathological analysis of post-mortem brain tissue of AD patients has shown typical biological traits that are present in most diagnosed patients, particularly amyloid- β (A β) plaques and neurofibrillary tangles (NFT) from the hyperphosphorylated protein tau (Lansdall, 2014). AD presents several cognitive domains which are apparent when the disease reaches severe stages rather than in mild cases, such as memory and social impairment. Given the failure of recent clinical trials, it is of importance to better comprehend the cellular mechanisms and proteins/genes implicated in AD, in order to advance treatment. Recent studies have shown that the protein RE1-silencing transcription factor (REST) has been strongly implicated in AD.

1.1 REST and Alzheimer's disease

REST is a transcriptional repressor, which acts by means of epigenetic modelling to silence target genes. Within neural progenitor cells, REST binds to the neuron-restrictive silencer element (NRSE) site in target genes prior to recruiting corepressors such as CoREST (Ballas *et al.*, 2001), which then enrol the enzymes histone deacetylases (HDACs) – 1 and 2 (Hwang, Aromolaran and Zukin, 2017; Hwang and Zukin, 2018). HDACs remove acetyl groups ensuring that the core chromatin complex is tightened, thereby, silencing the gene. This mechanism restricts access to the transcriptional machinery needed for the activation of genes at the promoter regions. Reports focusing on the expression of REST, show that REST expression is low in neural tissues, but expression is greater in non-neuronal tissues (Wu and Xie, 2006). A study reports on the importance of REST in development, as evidenced by the lethality of *Rest* KO mice. They show that REST is necessary to repress endogenous target genes in non-neuronal tissue (Chen *et al.*, 1998). Further reports demonstrating the function of REST suggests its importance in adult neurogenesis. A study by Gao *et al.*, 2011 showed that deletion of REST in adult neural stem cells generates an increase in neurogenesis. This work categorises REST as an adverse regulator of adult neural stem cell. In contrast, a dysregulation of REST has been associated with neurodegenerative disease (Lu *et al.*, 2014). This research explored the role of REST in AD which revealed high levels of REST in the brain of healthy elderly individuals but not in the brain of AD patients. This literature has methodically demonstrated that REST is a principle feature of neuronal aging in the hippocampus suppressing target genes which are involved in neuronal death. Respectively, they report that in elderly patients with normal cognitive preservation, there was

no dysregulation of REST as high levels were seen in the nuclei of cells. The level of REST was found to be depleted as there was a loss of REST in the nucleus in AD cases as well as in mild cognitive impairment (MCI); however, it was found that this was localised in neural regions such as the hippocampus. In contrast, no reduction was observed in nuclear REST levels in the cerebellum and dentate gyrus. Given these findings, the importance of REST preservation and normal regulation of REST is established.

REST has been identified in neuronally derived exosomes in blood. Foregoing research examined REST levels in four groups of patients: healthy elderly patients, MCI but were stable, MCI which lead to dementia and AD patients. Analysis of REST levels suggested a strong decline with an increased risk of AD or cognitive impairment (Ashton *et al.*, 2017), implying that those patients with a greater AD deterioration displayed lower levels of REST compared to those with MCI. Despite those findings, it remains unclear whether the levels of REST measured in peripheral blood in their study reflect the levels in the central nervous system. Supplementary research which similarly explored the relationship between REST levels and cognitive impairment using a blood-based approach, reported that levels of REST plasma protein were significantly lower in AD diagnosed patients (Marchant *et al.*, 2015). Even though, a dysfunction in REST in plasma neuronal exosomal levels in AD patients is already known, Abner *et al.*, (2016) examined this over a significant period in cognitively healthy elderly patients. Analysis of data suggested that exosomal protein levels for REST changed significantly with aging, although this was found to be observed outside of the range for AD patients. To elaborate, even though the levels of REST decreased with increasing age, levels remained higher in those who were cognitively healthy than those with AD.

Despite studies proposing reduced REST expression in AD, other reports focused on an alternative dysregulation in REST when associating the transcriptional repressor to choline acetyltransferase (ChAT) (González-Castañeda *et al.*, 2013). Formerly, dysfunctions in the molecular mechanisms for ChAT have been characterised as early distinctive features in AD, thus, implying that the relationship between ChAT and AD is a greatly understood field. Specifically, it has been shown that there is a decrease in ChAT expression in brain regions known to be affected in AD (Geula *et al.*, 2008), and it has been clarified that this reductive effect in ChAT levels was seen in patients diagnosed with AD (Heese and Akatsu, 2006). However, opposing levels of ChAT have been shown when associating the enzyme to REST. Reports have demonstrated that high levels of ChAT are correlated to a reduction in REST (González-Castañeda *et al.*, 2013). In a like manner, a study by Orta-Salazar *et al.*, 2012 strengthens the association between ChAT and REST expression by evaluating this protein expression using a triple transgenic mouse model of AD (3xTg-AD). They presented a reduction in ChAT cells in the hippocampus. Focusing on a region of the hippocampus known as the *Cornu Ammonis* 1

(CA1), high levels of REST were observed, this demonstrates the effect an increase in levels of REST has on ChAT levels and suggests its importance in neurodegeneration. Considering the dependence of REST on choline acetyltransferase, an increase in REST is thought to be a mechanism that initiates overexpression of proteins and an accumulation of A β involved in neurodegeneration.

By examining its functional consequence, a preservation of REST in the nucleus seems to avoid the development of dementia, there is, however, no published evidence to date associating REST with memory. This intriguing finding seems to suggest that typical biological traits of AD, such as neurofibrillary tangles and senile A β plaques, alone could not be sufficient to cause such progression of disease.

1.2 Immediate early genes (IEGs) and their regulation in memory

IEGs and their regulation by the cAMP response element-binding protein (CREB) are strongly implicated in the molecular mechanisms underlying memory formation (Kandel, 2012). A significant reduction in the expression of IEGs such as *c-fos*, *Egr-1 (Zif268)*, *Arc* and *Npas4* in the neocortex and hippocampus has been previously observed at the RNA level in the brain of *Rest* cKO mice (unpublished data). Thus, it is important to investigate not only the neurodegenerative pathology REST may present in AD cases, but also to explore whether the protein levels of immediate early genes are altered aiming to explain the memory impairment phenotypes in AD.

The signalling of the CREB is thought to have a crucial role in cognitive function. Research proposes that alterations in synaptic plasticity, which are due to CREB signalling, aid the translation of short-term memory to long term memory (Saura and Valero, 2011). For this reason, CREB is thought to be a fundamental protein for several biological mechanisms which are triggered during memory formation. Previous literature, which examined the level of CREB expression in AD models, reported that the expression of CREB mRNA was reduced in APP transgenic mice (Tg2576) (Pugazhenti *et al.*, 2011). Besides this, with the aid of histological analysis, they established that this change was concentrated mostly in the hippocampus and cortex, suggesting CREB expression is region specific. Alluding to the fact that dysregulated CREB expression is only seen in some neural regions, when focusing on post-mortem samples, a reduction was observed in the hippocampus. CREB is phosphorylated during memory processes, which is thought to initiate the transcription of memory associated genes. CREB mediated gene expression seems to be impaired in AD models. Reports by Echeverria *et al.*, (2004), have demonstrated that active forms of CREB kinase generally decrease in AD mouse

models. In the same way, other studies have reported a decrease in phosphorylated CREB in hippocampal neurons (Gong *et al.*, 2004), and in the prefrontal cortex of AD patients (Bartolotti, Bennett and Lazarov, 2016). Given the changes observed in CREB and phosphorylated CREB in AD patients and given the important role CREB has on regulating the transcription of immediate early genes, dysregulations are to be expected when investigating neurodegeneration.

The immediate early gene *c-fos*, is essential for synaptic plasticity and memory. Research proposes that this is focused on brain regions such as the hippocampus (He, 2002; Fleischmann *et al.*, 2003). *c-fos* activity is thought to be biphasic, increasing following acute neuronal activity but decreasing after chronic neuronal activity (Calais *et al.*, 2013; Renthal *et al.*, 2008). Studies have shown that when there is a decrease in the C-FOS expression it will provoke hippocampal cognitive deficits in AD mouse models (Palop *et al.*, 2003; Chin, 2005; Espana *et al.*, 2010; Corbett *et al.*, 2017). The immediate early gene, *c-fos* has been linked to the development of apoptosis in cultured neuronal cells (Estus, 1994). A study reports on the expression of C-FOS in hippocampal neurons, which forms part of the apoptotic pathway, in the CA1, CA2, CA3 and CA4 region of the hippocampus in AD patients. Findings demonstrate that abnormally high levels of C-FOS expression (Smeyne *et al.*, 1993) in sympathetic neurons appears to be a late event in apoptosis (Marcus *et al.*, 1998). The contradictory findings seem to imply that a dysregulation of C-FOS, by being either a reduction or increase play a role in neurodegeneration, suggesting that preservation of normal levels of C-FOS may be the best.

The phosphorylation of CREB as well as the recruitment of transcription factors initiate the transcription of genes such as *Egr-1*. Research by Bartolotti *et al.*, (2016) show that EGR-1 (*zif268*) expression is reduced in the CA1 region of the hippocampus in AD patients. Further research by Bonzon *et al.*, 2002, suggests that decreasing levels of the zinc finger protein 225 affect memory recall and spatial learning. Similarly, they reported that when using *zif268* mutant mice for behavioural tasks, specifically when examining the exploration time in the presence of novel and familiar objects, there was a level of difficulty in conserving information which had been retained over a period of 24 hours. Suggesting the importance this immediate early gene has on memory formation, and how cellular reductions of this protein could enable memory impairment. Literature which seems to suggest that EGR-1 is upregulated in AD mouse models, led scientists to examine the effect of silencing the transcription factor. The study by Qin *et al.*, (2017) demonstrated that when silencing of *Egr-1* occurs in the hippocampus it significantly improves cognition in the triple-transgenic mouse model of AD (3xTg-AD). It also seems to suggest that it plays a role in improving other characteristics involved in AD such as reducing the phosphorylation of tau.

Reduced levels of the immediate early gene *Arc* seem to be related to cognitive impairments. In contrast to the rest of the IEGs explored whose roles are transcription factors, *Arc* is the only one which is an activity-regulated cytoskeleton-associated protein. *Arc* is generally expressed in the hippocampal and cortical glutamatergic neurons and is required for several processes involved in memory such as preservation and strengthening (Guzowski *et al.*, 2000), but also it was proposed to be important for spatial learning (Plath *et al.*, 2006). A study focusing on this immediate early gene, used a mouse model with an overexpression of the destabilised yellow fluorescent protein Venus, which acts under the command of the *Arc* promoter at 7.1kb (*Arc::dVenus*). Findings of the study demonstrated a decrease in the expression of ARC in both hippocampal and cortical regions (Rudinskiy *et al.*, 2012). With regards to the DG, a study using human amyloid precursor protein transgenic mice (hAPP) reported that ARC expression is decreased in granule cells (Palop, 2005). Together, these studies imply that a dysfunction of ARC expression could contribute to the cognitive phenotypes observed in AD such as memory loss.

Being able to directly regulate the expression of many activity dependant genes, Neuronal Per-Arnt-Sim (PAS) domain-containing protein 4 also known as *Npas4*, has been identified as being important in memory (Lin *et al.*, 2008). NPAS4 is expressed preferentially in neurons and its expression is repressed by the attachment of REST to the promoter region of the *Npas4* gene (Bersten *et al.*, 2014). Comparing wildtype mice to a transgenic mouse model that expresses the human amyloid precursor protein (APP) conveying the Indiana and Swedish mutations (McGill Thy1-APP), a study by Duran *et al.*, 2013, found that the NPAS4 protein expression was lower in an Alzheimer's mouse model. Similarly, they report that as the mice aged, the expression of NPAS4 continually decreased further. When this finding was compared to the results obtained which explored long term potentiation (LTP), which is generally defined as a persistent strengthening of synapses, a decrease in LTP was associated with lower expression of NPAS4. When *Npas4* was inactivated from the CA3 region of the hippocampus in conditional knockout mice, it resulted in a cognitive deficit of long-term memory formation. On the other hand, overexpression of *Npas4* in the CA3 restored memory formation (Ramamoorthi *et al.*, 2011). Together the studies suggest the importance of non-dysregulated protein expression of NPAS4 for memory.

Considering both ARC and NPAS4, a study showed the importance that both immediate early genes have on memory (Qiu *et al.*, 2016). Following the use of the two trial Y-maze task, measuring spatial memory and real-time quantitative reverse transcriptase polymerase chain reaction (RT-PCR), a reduction was found for both IEGs in the hippocampus of mice with a level of memory impairment. However, the rodents who did not seem to have the cognitive impairment had normal levels of the proteins. This study also suggests that the lower expression of *Arc* and

Npas4, which is due to a dysregulation in the memory pathways, acts as an aid for the cognitive deficits seen in mice with the memory impairment.

Despite the association already established between REST and the IEGs, the enzyme histone deacetylase 2 (HDAC2) is similarly as vital with regards to REST. HDAC2 is an enzyme responsible for the removal of acetyl groups from the lysine residues on the histone proteins, which in turn contributes to the transcriptional silencing of genes (Kamarulzaman *et al.*, 2017). HDACs catalyse deacetylation of histones and many other nonhistone proteins such as CREB (Minucci & Pelicci, 2006). As such, it plays an important role in gene expression by circumventing the formation of transcription repressor complexes. A study reported the importance of regulated levels of HDAC2, suggesting an overexpression of HDAC2 assisted in an impairment in memory formation (Guan *et al.*, 2009). The findings in this study could help with understanding the association between REST and memory.

1.3 Morphological characteristics in neurodegeneration

Histological analysis can be undertaken to assess the morphological characteristics to evaluate the possibility of neurodegeneration in the brain of *Rest* cKO mice. Microtubule-associated protein 2 (MAP2) is thought to have a role in determining and stabilizing the structure of dendrites. Research by Huber and Matus (1984) suggests that MAP2 is generally confined within the dendritic arbor. As it is vital to understand the function of MAP2 in both neurodegenerative and normal conditions, a study carried out by Woolf, Zinnermann and Johnson, (1999) primarily demonstrated the importance of MAP2 for contextual memory. It was established that there was an increase in MAP2 in the hippocampus of rats a couple of weeks after training. Through analysis of transgenic and wildtype mice, the levels of MAP2 protein are demonstrated to decrease when there is a significant level of dendritic spine loss (Kandimalla *et al.*, 2017). Literature by Gonzalez-Lima (1998) on predictive markers of neurodegeneration demonstrate a continual decrease in MAP2, as well as a reduction of the apical dendrites specifically located in the CA1 region of the hippocampus. This is suggestive of a dysfunctional pathway due to neurodegeneration. In summary, it has been observed that neurodegeneration is associated with a reduction in levels of MAP2 protein and dendritic activation.

Synaptic loss is regarded as an early hallmark of AD. Previous literature reports that different levels of memory impairment are due to different levels of synaptic dysfunction or loss (Selkoe, 2002). Located in synaptic vesicles, the glycoprotein, synaptophysin can be used to observe changes that lead to synaptic loss (Gylys *et al.*, 2004). Using synaptophysin as a marker would establish any possible functional and distributional differences in synapses in *Rest* cKO mice

compared to controls. A study seems to report that as AD progression occurs, synaptophysin expression levels significantly decreased (Poirel *et al.*, 2018). As alterations in the post-synaptic structure have been identified in AD (Glylys *et al.*, 2004), it is important to associate this with disease progression. A study reports that even those with mild cognitive impairments harbour significant synapse loss (Scheff *et al.*, 2007), implying that this could be an indicator for cognitive decline. To further investigate synaptophysin as a marker of synaptic terminal levels, a report by Saura *et al.*, (2004) demonstrated reduced synaptophysin immunoreactivity in presenilin null mice, specifically in a *PS* cDKO model when compared to controls. Taking this study into consideration determines that a significant difference can be seen when there is a strong neurodegenerative phenotype.

Glial activation greatly depends on the development and severity of neurodegenerative disease. Neurons generally activate glia such as astrocytes using modulators such as glutamate (Liu *et al.*, 2006, Verge *et al.*, 2004). As such, following their activation, astrocytes alter the function of neurons and contribute to disease development such as AD. Reactive astrocytes are a prominent feature of AD, but their role in AD is not fully established. Comparing the difference in astrocyte structure, a study found that the astrocytes in those with AD pathology but who had normal cognition seemed to have longer and thicker processes (Kobayashi *et al.*, 2018). To create a better understanding this finding was compared to those patients with AD pathology but who also had dementia, in which shorter and thinner processes were seen. Further literature which seems to suggest that changes in astroglia in aging and neurodegenerative disease are heterogenous, demonstrate functional astroglial traits. The study also seems to propose that astrocytes themselves undergo degeneration in the early stages of pathological progression. By further analysis of astroglia in later cases of disease progression, astrocytes were found to be associated with neurite plaques. The given research seems to suggest this is located in specific brain regions rather than the astroglia being scattered, as it was seen in regions such as the hippocampus but not in neural regions such as the Entorhinal cortex (EC) (Rodriguez – Arellano *et al.*, 2016). Astrocytes tend to be focal in AD cases, such that the reactive astrocytes are closely associated with A β plaques and surround them with dense layers of astrocytes, almost forming a wall and acting as a neuroprotective barrier. Of interest, some studies seem to report that reactive astrocytes can absorb and then degrade deposits of A β (Wyss-Coray *et al.*, 2003), which recommends that the dysfunctions in the reactive astrocytes could have a role in the development of disease. When aiming to morphologically observe astrocytes, using immunohistochemistry, the glial fibrillary acid protein (GFAP) has been reported to be a typical marker (Sofroniew and Vinters, 2010).

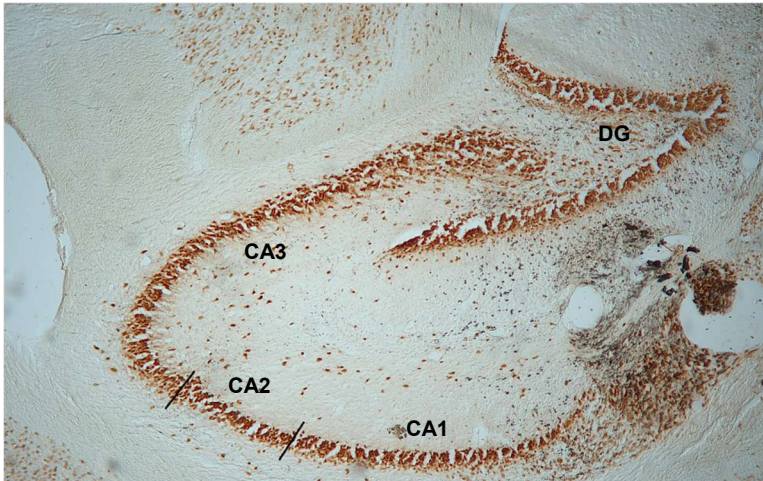


Figure 1

The regions of the hippocampus identified

Labelled are the different regions of the hippocampus studied. The CA1, CA2, CA3 and DG are identified following immunohistochemistry staining with NeuN, a neuronal nuclei marker. The image was taken at 5x magnification.

1.4 The CA2

The hippocampus is crucial for memory, and the function of further sub regions such as the CA1, the CA3 and the DG have been extensively explored. A sub-region of the hippocampus, known as the CA2 has been relatively overlooked (Mou, 2016). The CA2 pyramidal neurons possess distinctive physiology that distinguishes them from CA1 and CA3 neurons (Chevaleyre and Piskorowski, 2016). Recent literature has indicated that social memory is an attributed function of the CA2 area of the hippocampus (Hitti and Siegelbaum, 2014; Benoy, Dasgupta and Sajikumar, 2018). The properties of the CA2 pyramidal neurons involve specific action firing patterns. Elaborating on these firing patterns, a study by Ochiishi *et al.*, (1999) revealed that individual CA2 cells display similar firing patterns to that of the CA1 and CA3 by using *in vivo* recordings in rats. However, it differs from the other two sub-regions in that the CA2 cells do not maintain their spatial coding and carry less spatial information (Mankin *et al.*, 2015; Lu *et al.*, 2015). Structurally observing the CA2 region, it is clear that it is more neuronally dense and has fewer oblique dendrites than the CA1. Correspondingly, in the CA2 the apical dendrites which are present in the pyramidal neurons specifically in mice, are branched in a unique manner which suggests they are suitable for transmitting signals to the cell bodies from its distal synapses (Dudek, Alexander and Farris, 2016).

Perineuronal nets (PNNs) are unique extracellular matrix structures that sheathe the neurons in the central nervous system (CNS) during development, besides controlling the plasticity in the adult CNS (Horii-Hayashi *et al.*, 2015). PNNs are recognised as being able to contribute to a wide variety of disorders including learning and memory (Sorg *et al.*, 2016). This field of research has been explored intensely, and results demonstrated that PNNs surround CA2 pyramidal neurons (Carstens *et al.*, 2016; Lensjo *et al.*, 2017), demonstrating their dense expression. Due

to restricting the synaptic plasticity at hippocampal synapses, PNNs could be responsible for having a key role in memory impairments.

The novel discoveries on the properties of the CA2 have allowed a greater understanding on the role of the CA2 in social memory. The functional and structural qualities have been approached in a variety of research which has produced concluding findings on the importance of the CA2 in social memory.

1.5 The role of the CA2 in social memory impairment

The role of the CA2 in social memory has been explored using studies which genetically modify pyramidal neurons by silencing genes in the CA2 or alternatively, introducing lesions in the CA2 hippocampal area. Literature by Alexander *et al.*, (2016) showed the importance of the CA2 for being responsible for social memory. When presenting a social stimulus to mice models, varying between a novel and familiar littermate, this induced the global remapping of place fields in only the CA2 region of the hippocampus. A place field is a specific location in an animal's environment where excitatory pyramidal neurons called place cells fire (Sheffield and Dombeck, 2019). Thus, these findings suggest that the CA2 is involved in encoding social and novel contextual information.

Modification by lesioning the CA2 pyramidal neurons can be approached to explore the effect of a dysfunctional CA2 region in social memory (Stevenson and Caldwell, 2014; Hitti and Siegelbaum, 2014). Stevenson and Caldwell, (2014) delved into this by using rat models by injecting N-methyl-D-aspartate (NMDA) in the dorsal CA2 which fabricated a lesion. Implementing behavioural studies such as the two-trial social discrimination test and the hidden cookie test, the research was able to conclude that excitotoxic NMDA lesions of the CA2 impair social recognition memory. Reports by Hitti and Siegelbaum, (2014) used both genetic silencing and lesioning of the CA2 to substantiate its influence in social behaviour. They described that the selective silencing of the CA2 did not change sociability as both groups demonstrated a like preference for the chamber with a littermate using the three-chamber test of sociability. On the other hand, they showed that the synaptic transmission in the CA2 was blocked. Thus, they suggest that the two different forms of modification produced different outcomes. Concluding on these two studies, the most effective method to analyse social memory in the CA2 occurs by introducing lesions which alter the biochemical processes allowing the behavioural phenotype to arise.

It may be useful to analyse the CA2 in a mouse model such as *Rest* cKO, which has a phenotype that possibly includes social memory elements.

1.6 Protein involvement in social memory impairment

To gather a greater understanding on the effect that diverse levels of vasopressin in the CA2 exhibit in relation to social memory, Smith *et al.*, (2016) employed an optogenetic technique to stimulate vasopressin terminals. Conclusions on the findings, emphasised the importance of the CA2 and the vasopressin 1b receptor (V1BR) for memory and social behaviour. Confirmation of this idea is found in behavioural reports using V1Br knockout (KO) mice which show that these mice display reduced social memory (Wersinger *et al.*, 2002; DeVito *et al.*, 2009; Chevalayre and Piskorowski, 2016). Regardless of such results, *in situ* hybridisation experiments by Young *et al.*, (2006) demonstrated that vasopressin v1b mRNA is located outside of the hippocampus. When this is dysregulated or deleted it produces non-hippocampal dependent behaviours, involving a reduction in social memory, which clearly questions the selective role of the CA2.

A depletion in the levels of oxytocin causes deficits in social memory. Research which explores levels of oxytocin in perinatal stages, identified that a disruption in oxytocin levels is thought to interact with the establishment of the cortex and numerous callosal connections (Zhang *et al.*, 2016). Using mice which had unilateral transection of the infraorbital nerve (ION-transected), behavioural tests were employed to explore any behavioural deficits which may be present. The research determined that the mice had deficits in their social and spatial memory when compared to control mice models. They established that this deficit in social memory was correlated to lower levels of oxytocin in the hypothalamus suggesting its importance in behavioural depletions. Of similar relevance, Raam *et al.*, (2017) suggested that oxytocin receptors (OXTRs) in the anterior CA2 and in the distal CA3 are obligatory for social stimuli. By analysing OXTRs expression, results determined an enrichment in the anterior CA2 and distal CA3 regions. However, this level of expression of OXTRs was generally always present in the CA1 and anterior CA3 regions. The expression of oxytocin, its receptors and their importance in social behaviour has been further confirmed by Lin *et al.*, (2017). This research focused on OXTRs expressed in the hippocampal pyramidal neurons specifically in the CA2 and CA3. When using conditional knockout mice, the research demonstrated the importance of normal regulated levels of OXTRs for excitatory neurons in the CA2 and CA3 regions. The results obtained showed a dysfunction in the forebrain and associated hippocampal regions. This deletion in the receptor suggested a restriction to the excitatory neurons in the adult mice, which caused a deficit in their

long-term social recognition memory. Concluding, a downregulation of the levels of oxytocin receptor protein or oxytocin alludes to deficits in social memory related behaviours.

Another protein that has shown relevance when analysing memory through the CA2 region of the hippocampus is corticotrophin releasing factor (CRF). Since CRF gene expression is involved in memory processing, an overexpression of the respective protein enables better social recognition memory (Kasahara *et al.*, 2010). Using transgenic CRF over-expression (CRF-OE) mice and comparing them to wild type controls, the CRF-OE seemed to demonstrate better social interaction and normal short-term memory, enlightening the importance high levels of CRF have on memory. Moreover, it suggests that those with reduced levels could present with a memory impairment phenotype. Ma *et al.*, (1999), similarly demonstrated that when CRF is injected into the dentate gyrus of the hippocampus, the performance of rodents is increased during an inhibitory avoidance learning task. Furthermore, literature relating CRF levels and AD show that a deficit in CRF contributes to cognitive impairment (Behan *et al.*, 1995). The literature on CRF and memory impairment overall indicates how important high levels of CRF are for normal cognition. Using an alternative approach to investigate levels of CRF, a study by Korosi *et al.*, (2010) suggests that maternal care represses stress responses and helps improve cognitive function. The study by means of rat pups which received augmented maternal care, demonstrated reduced synaptic currents onto CRF neurons. When comparing the levels of CRF with REST, they found that REST negatively regulates the transcription of the *Crf* gene. Considering this study, it demonstrates that early life experiences amend gene expression. When relating this experience related plasticity to the molecular mechanisms understood in this study, it provides a platform in understanding behaviour with regards to protein dysregulation. Similarly, this study also approaches the association between REST and CRF, confirming the important role REST has in regulating several different genes and proteins.

1.7 A novel behavioural phenotype in *Rest* cKO mice

A repetitive memory impairment phenotype has been previously observed by the supervisor of this present study during behavioural investigation of *Rest* cKO mice (unpublished data), employing experimental systems such as the object exploration task. A possible hypothesis is the presence of a typical neurodegenerative phenotype. The literature which comprises of similar behaviours seen in conditional knockout rodents, suggests another possible hypothesis to explain the behavioural phenotype. Rather than being a neurodegenerative trait it could better be explained by similarities to obsessive-compulsive disorder (OCD) (Witkin, 2008; Angoa-Perez *et al.*, 2013).

1.8 Experimental aims

Collectively, all of the literature on REST involvement in neurodegeneration initiates a bigger role that needs further clarification. Therefore, it is of utmost importance to further enlighten the molecular mechanisms behind its association with AD. This study aims to take some of the next steps in this direction. It also aims to investigate the previously suggested role of REST in regulating neuronal survival (Lu *et al.*, 2014) in an experimental system not previously used for these purposes, possessing the following advantage. Inactivation of *Rest* in the mice used in this study takes place postnatally (age: 2-3 weeks), avoiding potential developmental abnormalities. This will be investigated through the use of western blot experiments, analysing antibodies of interest to memory. Similarly, investigating the number of neuronal nuclei between *Rest* cKO mice and controls in the CA1, CA2, CA3 and DG region of the hippocampus to be able to explain the role of REST in neurodegeneration.

Methods

2.1 *Rest* conditional knockout mice

For the purpose of this study conditional inactivation of *Rest* in *Rest* cKO mice was achieved using of the Cre-lox system, by breeding “Floxed” *Rest* mice with CaMKIIa-Cre transgenic mice. In “Floxed” *Rest* mice, Exon 2 of *Rest* (the first coding exon) is flanked by loxP sites. In CaMKIIa-Cre transgenic mice (Minichiello *et al.*, 1999), Cre recombinase is expressed under the control of the CaMKIIa promoter, which confers specificity of Cre expression and therefore *Rest* inactivation in excitatory neurons of the postnatal forebrain (beginning in 2-3 weeks of age) bypassing the embryonic lethality caused by germline REST inactivation (Chen *et al.*, 1998). Both the *Rest* cKO and control samples were collected from a colony of mice in Edinburgh. The mice were perfusion-fixed, before the brains were collected. Before collection of brain samples, they were fixed with paraformaldehyde to preserve the structure. This fixation procedure applies only to the brains used for histology/immunohistochemistry. Tissue samples were frozen with cryo-embedding medium, and then stored at a temperature of -80°C. Both the left and right hemispheres were used for analysis. Mice used were balanced for gender. All procedures were performed blindly.

2.2 Cryostat sectioning

The brain tissue which was embedded in optimal cutting temperature (OCT) medium was taken out of the -80°C freezer. This sectioning procedure involved adhering the frozen mouse brain

hemisphere to the cryostat platform with the use of OCT, a liquid at room temperature. Once this was assembled, it was quickly placed into the cryostat to freeze. The cryostat platform was then inserted into the correct position on the cryostat prior to adjustments being made on the angle and distance from the blade. Sagittal sections were cut before being mounted onto gelatin-coated glass slides. Sections were cut at a thickness of 30µm. 3 sections were mounted onto one glass slide. The slides were left at room temperature for a short duration so they could air dry. They were then stored in a freezer at -20°C.

2.3 Haematoxylin staining

Sections were taken out of the -20°C freezer and left to dry at room temperature for 20 minutes. A hydrophobic pap pen was used to circle the sections, ensuring the reagents did not leak from the slides. Sections were hydrated with distilled H₂O for 5 minutes before being incubated in Harris' haematoxylin dye for 1 minute to stain the nuclei of cells. A further application of distilled H₂O twice for 5 minutes was applied to eliminate any background staining. Sections were incubated in tap H₂O for 5 minutes. Sections were then placed in a series of dilutions of industrial methylated spirits (IMS) or ethanol as part of the dehydration stage. Sections were left in 50%, 70%, 90% and 100% alcohol for 3 minutes each prior to being placed in histoclear for 3 minutes. Sections were then mounted with histomount, coverslips were positioned, and the slides were left to air dry.

2.4 Cresyl Violet (Nissl) staining

Sections were taken out of the -20°C freezer and were left to dry at room temperature for 20 minutes. A hydrophobic pap pen was used to circle the sections. Sections were hydrated with distilled H₂O for 5 minutes, before being incubated with filtered cresyl violet for 5 minutes. The sections were then washed 2 times for 5 minutes each with distilled H₂O. In order to dehydrate the sections, they were placed in industrial methylated spirits (IMS) or ethanol for 7 minutes until most of the stain was removed. They were then incubated in an organic solvent similarly used for the dehydration step, histoclear, for 5 minutes, before mounting with histoclear and coverslips. Sections were left at room temperature to dry before observations.

2.5 Immunohistochemistry

Sections were air-dried for 15-30 minutes prior to use. Sections were hydrated in PBS for 7.5 minutes. An incubation using 0.5% triton was done for 10 minutes. This pre-treatment of triton, a detergent, is responsible for breaking down the cell membrane. Thus, it was used to give the antibody better access to the cell. Then, another incubation of PBS for 7.5 minutes. A quenching incubation of 0.3% of hydrogen peroxide (H_2O_2) and 100% methanol, was applied to occlude any endogenous peroxidase activity, for 15 minutes, prior to another PBS wash (7.5 minutes). An incubation of 0.5% of Normal-Goat Serum (NGS), for 30 minutes at room temperature was applied on the sections, prior to the primary antibody being added in the same block solution which was left for 1 hour at room temperature. Two washes with PBS were then undertaken (7.5 minutes each). Using the appropriate goat or horse biotinylated secondary antibody, 13.5 μ l of antibody was added to a total volume of 3ml block. This was an incubation of 30 minutes at room temperature. Repeatedly, a further two washes with PBS were undertaken (7.5 minutes each) after the secondary. Halfway through the secondary antibody incubation, the Avidin-Biotin (AB) complex was prepared which intensifies the target antigen signal using the VECTASTAIN ABC-AP staining kit. The complex consisted of 2.5ml PBS, 25 μ l serum, 25 μ l of reagent A and reagent B and was left for 30 minutes at room temperature. Two washes with PBS for 7.5 minutes each followed this. Sections were incubated in DAB for 8 minutes using the DAB Peroxidase (HRP) Substrate Kit. This consisted of 2.5ml distilled H_2O , 1 drop buffer, 2 drops DAB stock and 1 drop hydrogen peroxide (H_2O_2). Following this, two washes with PBS for 7.5 minutes each. The haematoxylin counterstain (700 μ l per slide, incubated 5 minutes), was sometimes applied which was followed by: distilled H_2O incubation for 3 minutes, tap water for 5 minutes, and distilled H_2O incubation for 3 minutes. The dehydration stage involved ethanol (or IMS) at concentrations of 50%, 70%, 90% and 100%, sections were incubated in each for 3 minutes before an incubation in histoclear for 3 minutes. Sections were then mounted with histomount and coverslips before leaving to air dry.

2.6 Citrate Antigen Retrieval

Sections were incubated in PBS for 7.5 minutes before the quenching step occurred and the sections were put in a mixture of hydrogen peroxide (H_2O_2) and methanol for 15 minutes followed by another PBS wash for 7.5 minutes. Using the Dako PT link instrument, sections were prepared for the antigen retrieval process using a water bath. The solution of the selected target retrieval stock solution was prepared (10x). This involved 3.78g of citric acid in 180ml distilled H_2O and 24.11g of Tris Sodium Citrate in 820ml distilled H_2O . Both of these solutions were mixed and then stored at 4°C. The stock solution was diluted to 1x before use. If the citrate

solution was made previously it was checked to ensure it had not been used more than 3 times and that there was a total volume of 1.5L at pH. 6. The lid was placed on the tank, and the lid was closed and locked with an external latch so that the optimum temperature could be achieved. Antigen retrieval temperature was set to 97°C. Preheating temperature was set to 65°C. When the temperature reached 65°C, the PT link lid was opened and the sections were placed on the autostainer slide rack so that the sections were immersed into the preheated target retrieval solution, this was then run. Sections were left in the solution at 97°C for 20 minutes. When the cycle finished, the cooling stage began bringing the temperature back down to 65°C. The sections were then placed in hot tap water twice for 5 minutes. Then, put in PBS before the rest of the IHC protocol was conducted for staining of the sections.

2.7 Protein Lysate Preparation

Preparation of Neocortical lysate:

400µl of buffer A was added to the sample. Buffer A composition can be found in appendix A. The brain tissue was homogenised using the Fischer motor pestle for 5 minutes for 10 second intervals, resting the sample on ice in between. 600µl of buffer A was added to the sample before it was re-suspended. An aliquot was prepared of the homogenate (250µl) before a mixture of solutions were added. Concentrations were calculated considering the concentration of each component in buffer A. To the 250µl of homogenate, a series of reagents were added yielding final concentrations of: 0.04M Tris, 0.08M NaCl, 0.005M EDTA, 0.5% sodium deoxycholate and 1% SDS. The total lysate was rotated for 30 minutes at rpm 40 at 4°C on the Stuart Rotator SB3, before using the vortex for a total duration of 30 seconds for 5 second intervals, resting on ice in between. The total lysate was centrifuged at 14000 rpm for 10 minutes at 4°C in the Eppendorf centrifuge 5430 R before the supernatant was collected.

Preparation of Hippocampal lysate:

For both the neocortex and hippocampus, the same protocol was followed. Alterations were made to the volume of reagents when using hippocampal tissue due to there being a smaller quantity of tissue. A total of 400µl of buffer A was added for the homogenisation. When the aliquot was prepared for the homogenate (100µl) an additional 150µl of buffer A was added to the homogenate only. Regarding the nuclear extraction, 500µl of lysis buffer was added rather than 1.2ml. The quantities used for the phosphatase inhibitor cocktails were calculated taking the new volumes into account (1% phosphatase inhibitor cocktail 2 and 3 for buffer A, 0.5% phosphatase

inhibitor cocktail 2 and 3 for lysis buffer). In terms of experimental analysis only total cell lysate (homogenate) and nuclear extraction samples were used.

2.8 Nuclear Extraction

The remaining aliquot (750µl) from the homogenate preparation was rotated for 20 minutes at 40 rpm at 4°C on the Stuart Rotator SB3. The samples were vortexed for a total duration of 30 seconds for 5 second intervals, resting on ice in between. The sample was centrifuged at 1000g for 10 minutes at 4°C in the Eppendorf centrifuge 5430 R. The non-nuclear supernatant was collected. 1.2ml of lysis buffer was added to the pellet before it was re-suspended. The lysis buffer was prepared by mixing an equal volume of the RIPA buffer and the RIPA supplementary buffer. Lysis buffer composition can be found in appendix A. The nuclear prep was rotated for 30 minutes at 4°C at 40 rpm on the Stuart Rotator SB3 and then similarly vortexed for a total duration of 30 seconds, in 5 second intervals. The sample was then centrifuged again at maximum speed for 10 minutes at 4°C before the nuclear supernatant was collected. The kit which was used as part of the optimisation stage for the nuclear extraction, was obtained from abcam.

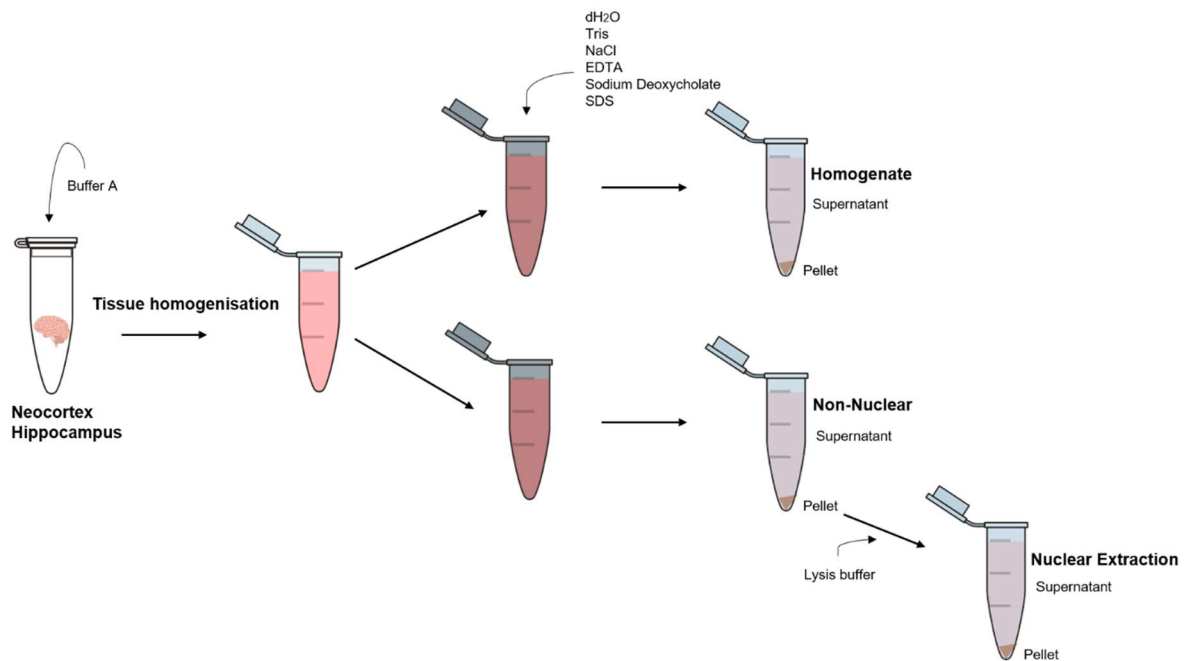


Figure 2

Homogenisation and Nuclear Extraction method

Seen are the general steps undertaken for homogenising the brain tissue and nuclear fractionation. Following homogenisation, for neocortical samples (250µl) or for hippocampal samples (100µl) was aliquoted for the homogenate and the remaining volume, for neocortical samples (750µl) or for hippocampal (300µl) was used for the non-nuclear and nuclear extraction.

2.9 Pierce BCA Protein Assay

In order to determine the total protein amount in the brain tissue the Pierce BCA method was approached. The protein standard was prepared using RIPA buffer and BSA. Several dilutions were prepared for the unknown total protein using RIPA buffer. 10µl of the protein was added to the appropriate wells in the transparent flat bottom 96 well plate and 100µl of the Pierce BCA protein assay reagents (A and B). The plate was covered in foil and incubated on the Stuart mini rotate shaker SSIM for 5 minutes before incubating in the Gallenkamp for 45 minutes at 37°C. Measurements were taken using the Genios Pro plate reader and software and calculations were undertaken.

2.10 SDS-PAGE Gel Electrophoresis

A combination of SDS sample buffer and DTT, along with RIPA buffer was added to the protein samples. The protein samples were vortexed for 10 seconds and then heated for 10 minutes at 75°C using the Techne DRI-BLOCK DB3 before loading in the lanes of gel. Gels were run at 200V constant at room temperature. The gels used were later changed thus did the running buffer. For the Bis-Tris gels (8-16%) Fischer Tris-Glycine running buffer with SDS (10x) was used, when the gels changed to NuPage 4-12% Bis-Tris, the Fischer MOPS (20x) running buffer was used. Either the full range rainbow recombinant protein marker or the precision plus protein dual colour standard were used as the protein standards throughout the research.

2.11 Activation of the PVDF membrane

For protein transfer from the gel, a PVDF membrane was used. After cutting the membrane to the appropriate measurements (5.5cm x 7.5cm), it was placed in methanol for 10 seconds. With the aid of forceps, the membrane was lifted to ensure excess methanol was removed prior to leaving in two washes of distilled water for 2-3 minutes each and then incubating in transfer buffer before use.

2.12 Wet transfer

The transfer cassette was assembled as appropriate using 2 sponges and 2 filter papers (so the current was able to run from the black side to the red) and inserted into the transfer tank with an ice block to maintain the temperature. Transfer buffer was prepared using the fisher transfer buffer (10x) and 20% methanol. An alternative transfer buffer which was used on a few occasions

involved 800ml distilled H₂O, 15g of glycine and 3g of Tris Base, similarly using 20% methanol. Transfer was run at 200mA constant for 2 hours at 4°C.

2.13 Trans-blot turbo semi-dry transfer system

The transfer system was obtained from Bio-Rad. 6 filter papers were used to encase the gel and membrane in the tray before it was inserted into the apparatus. The appropriate programme was set for a transfer time of 30 minutes, covering a range of molecular weights.

2.14 Western Blotting

The PVDF membranes were washed with PBS-Tween (PBS-T), derived from a 20x stock solution, for 5 minutes after transfer before they were incubated in 5% dry skimmed milk prepared with PBS-T for 1 hour at room temperature. The primary antibody was left to incubate over night at 4°C on the VWR rocking platform. Membranes were washed with PBS-T (1x), 3 times for 5 minutes, before the secondary antibody was incubated for 1 hour at room temperature and was left on the Stuart mini orbital shaker SSM1. All antibodies were prepared in 5% dry skimmed milk and PBS-T. Membranes were once again washed with PBS-T (1x) 3 times for 5 minutes prior to using the Enhanced Chemiluminescence (ECL) detection method. The ECL detection method involved mixing reagents A and B for 1 minute, then incubating on the membrane for 5 minutes.

2.15 Image Acquisition

For the purpose of image acquisition regarding the sections which were used for histology and IHC, the Leica DM2500 LED microscope was used with Leica Application Suite X (LAS X) software so that images of the whole hippocampus, the CA1, CA2, CA3 and DG could be taken. Magnifications used involved 5x for the whole hippocampus and then 10x for the individual regions. Images taken at 10x were used for quantification purposes. For some samples which provided difficulty upon quantification, images were then taken again at 20x for better resolution.

When imaging the membrane, from western blot investigation the Bio-Rad Chemi Doc molecular imager XRS camera was used along with the Image Lab 3.0.1 (β1) software. The appropriate signal accumulation mode was set up depending on the exposure of different antibodies. This was noted from previous experiments when optimisation took place. The Chemi setting was used

when imaging the protein bands and the Calorimetric setting was applied when imaging the standard. Both images were then aligned appropriately so the molecular weight (kDa) could be identified.

2.16 Quantification

When quantifying the sections which were used for histology and IHC, the appropriate region of the hippocampus was selected at 10x magnification. A group of 3 students blindly quantified the same image using clickers and then an average was calculated for reliability. When quantifying astrocytes, it was previously agreed on what would be classified as an astrocyte for example the number of processes the astrocyte consisted of (3 or more) and only those were counted.

For quantification of the western blot images, this was done using a software in the imaging system. An analysis table was produced which was then exported to excel. An average for the background was calculated and then deducted from all of the protein sample values. This same procedure was repeated for the loading control. When normalising the values, the densitometry value for the original protein band was divided by the appropriate loading control value. These readings were then used to make a bar graph with the normalised values of protein abundance.

2.17 Statistical analysis

Statistical analysis was run on sections used for histology and IHC and the western blot images following quantification of the protein bands. Two tailed t-tests and ANOVAS were undertaken.

2.18 Antibodies

Table 1

Antibodies used with the corresponding application and dilution

Listed are the antibodies used in the present study. Additional materials can be found in the table such as the use, species, application, company it was obtained from, catalogue number and dilution.

Antibody	Use	Species	Application	Company	Catalog No.	Dilution
Anti-Phosphorylated CREB	Primary	Rabbit	WB	Cell signalling technology	9298	1:2000
Anti-V1B receptor	Primary	Rabbit	WB	Abcam	ab104365	1:2000
Anti-Oxytocin receptor	Primary	Goat	WB	Abcam	ab87312	1:2000
Anti-Corticotrophin releasing factor (CRF)	Primary	Rabbit	WB	Abcam	ab8901	1:2000
Anti-Egr1	Primary	Rabbit	WB	Abcam	ab133695	1:2000
Anti-HDAC2	Primary	Mouse	WB	Abcam	ab12169	1:10,000
Anti-Arc	Primary	Rabbit	WB	Abcam	ab183183	1:2000
Anti-CREB	Primary	Rabbit	WB	Abcam	ab31387	1:1000
Anti-Npas4	Primary	Goat	WB	Abcam	ab109984	1:2000
Anti-cfos	Primary	Mouse	WB	Abcam	ab208942	1:2000
Anti-GFAP	Primary	Rabbit	IHC	Abcam	ab7260	1:4000
Anti-MAP2	Primary	Mouse	IHC	Abcam	ab11267	1:1000
Anti-NeuN	Primary	Rabbit	IHC	Abcam	ab177487	1:6000
Anti-Synaptophysin	Primary	Rabbit	IHC	Abcam	ab32127	1:1000
Anti-Synaptophysin	Primary	Rabbit	WB	Abcam	ab32127	1:100,000
Anti- β tubulin	Loading Control	Rabbit	WB	Abcam	ab6046	1:20,000
Anti- α tubulin	Loading Control	Rabbit	WB	Abcam	ab7291	1:10,000
Anti- β actin	Loading Control	Mouse	WB	Abcam	ab8226	1:5000
Anti-Histone H3	Nuclear Loading Control	Rabbit	WB	Abcam	ab1791	1:5000
Nuclear Extraction Kit				Abcam	ab113474	

Results

3.1 Nuclear Extraction Optimisation

Prior to data collection, the total lysate preparation and nuclear extraction protocols had to be optimised. For the nuclear extraction, two different protocols were tested. A kit from a commercial supplier and a general protocol from research gate. The results which can be seen in **figure 3**, show better separation from the general protocol than the commercial kit. The general protocol was then adapted before using on *Rest* cKO mice and controls.

CREB, a nuclear protein was used to see which nuclear extraction protocol was the most effective. By using the commercial kit, it is clear that the separation of the sample was not the best, as the band is seen in the non-nuclear fraction rather than the nuclear extraction. When observing the bands for the general method used, the protein band is seen in the nuclear extraction sample but not in the homogenate or non-nuclear, suggesting good separation. Synaptophysin was used as a non-nuclear marker.

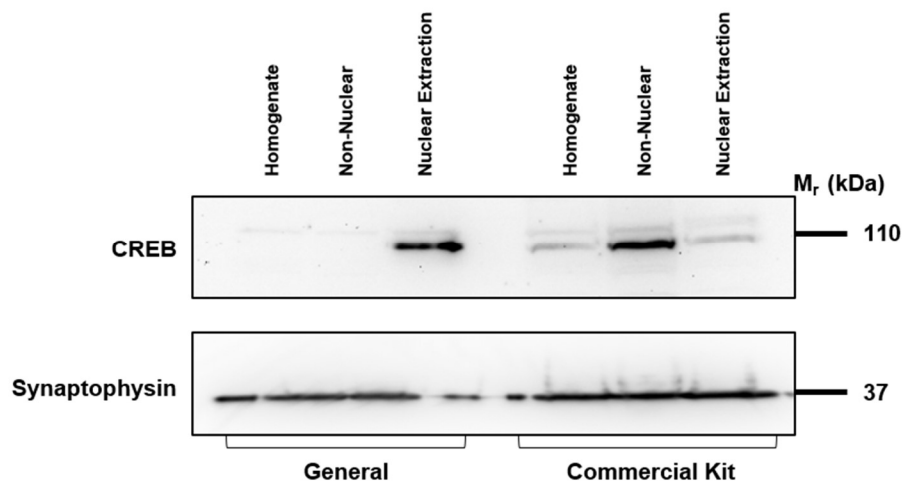


Figure 3

Determination of the efficiency of different nuclear extraction protocols

Imaged are two western blots, the first with the nuclear protein CREB and the second with synaptophysin as a non-nuclear marker. The bands for CREB appear at 110kDa, and the bands for synaptophysin are imaged at 37kDa. The first 3 columns from the left consist of the general protocol, with all homogenate, non-nuclear and the nuclear extraction samples. The later 3 columns show the separation of the samples using the commercial kit, similarly when using the homogenate, non-nuclear and nuclear fractions.

3.2 Antibody optimisation

Before data collection began, all antibodies which were going to be used had to be optimised in order to discover the optimal exposure time and dilution which would be most effective to use. Western blot experiments were undertaken using practice samples of the homogenate, non-nuclear and nuclear extraction fractions. **Figure 4a** and **4b**, shows the western blots obtained during optimisation. For most antibodies, bands at one molecular weight were seen, though for a couple of antibodies such as C-FOS and EGR-1, multiple bands are seen at various molecular weights. Given this, the loading controls were carefully selected to not interfere with background bands. See appendix B for antibody table with optimised antibody dilutions.

3.3 Testing the Trans-blot turbo semi-dry transfer system

When receiving the trans-blot turbo machine, prior to using it on *Rest* cKO samples, it was tested and compared to the traditional transfer method. As seen in **figure 4c**, both transfer methods seem to work well, the only difference was the amount of protein transferred. The standard transfer method seemed to transfer a lot more protein than the trans-blot turbo. The possible difference in exposure time was accounted for as both membranes from either transfer method were imaged simultaneously on the imaging plate. Thus, the trans-blot turbo transfer system was generally used for proteins with a short exposure time, for those with a longer exposure time for example 200-300 seconds, the standard transfer method was approached.

3.4 Testing PVDF membranes

Following the testing of the trans-blot turbo, membranes were then tested to see if there were any differences between the standard PVDF membrane or the PVDF membrane which came with the trans-blot turbo machine. By observing **figure 4d**, no major differences can be seen when comparing the two membranes, as both seemed to work well. For the GFAP western blots in **figure 4d**, the quantified values were used for the graphs seen in **figure 4e** and **4f**. The graphs allow the linear relationship to be observed, as 1, 5 and 20 μ g was loaded across all conditions. By analysing both graphs and observing the R^2 linear regression value, both graphs seem to show a strong linear relationship. When analysing the R^2 value the standard PVDF has a value of 0.999 and the trans-blot turbo PVDF of 0.9986 suggesting both have close proximity of the points to the regression line. Due to both membranes showing such high R^2 values, the standard PVDF membrane was chosen to be used in future experiments.

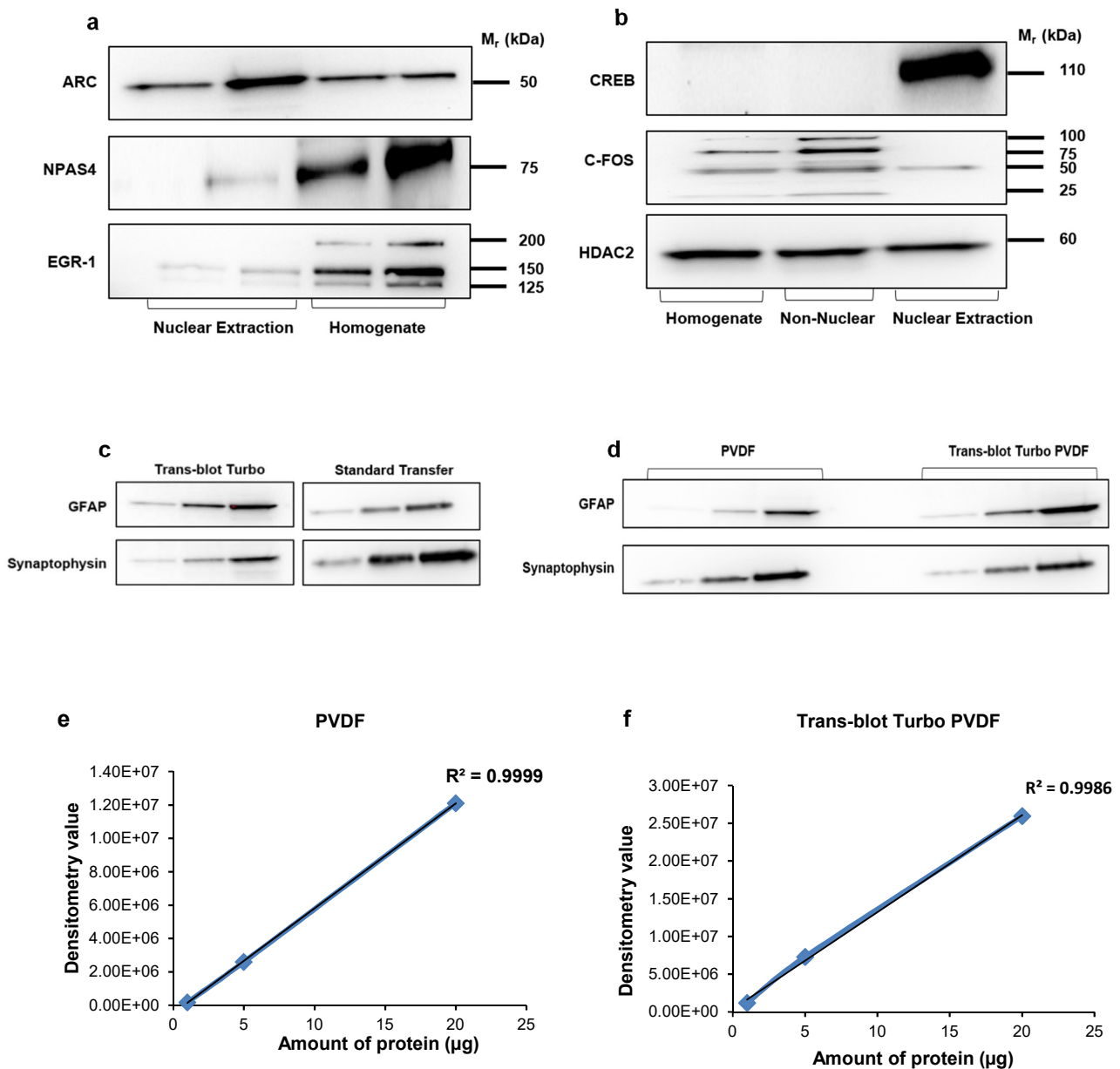


Figure 4

Optimisation of antibodies, transfer system and PVDF membrane

Imaged above are the western blots following during antibody optimisation. Bands are seen in all blots and those which only have bands at one molecular weight the blot was aligned with the standard in order to determine their molecular weight. ARC bands showed up at 50kDa, NPAS4 at 75kDa, CREB at 110kDa and HDAC2 at 60kDa. For EGR-1 and C-FOS, multiple bands were seen at different molecular weights. **a**, the first and third lane had 10µg of sample, and the second and fourth had 20µg of sample. **b**, for all samples 20µg was used. **c**, the optimisation of the transfer methods, samples involved 1µg of protein in the first well for all western blots, 5µg for the second well and 20µg for the third. The western blots imaged on the left are from the Trans-blot turbo, those on the right are the standard transfer. **d**, the optimisation of the PVDF membranes, sample amounts used are the same for those in **c**. The western blots on the left are those using the standard PVDF, on the right those using the TBT PVDF. **e**, represents the quantified values for the samples when the standard PVDF membrane was used. **f**, represents the quantified values when the Trans-blot turbo PVDF membrane was used. For both graphs **e** and **f**, values used for the graphs are from the GFAP western blots.

3.5 Pilot analysis of *Rest* cKO and control in homogenate and nuclear extraction samples

When comparing the amount of protein across *Rest* cKO and controls by using western blots, it was fundamental to have a method which accounts for variation in loading or protein transfer. Along with other traditional loading controls used such as α tubulin, β tubulin and β actin, Histone H3 was ordered to be used as a nuclear loading control for the nuclear extraction samples.

Analysis of homogenate and nuclear extraction samples show varied findings. CREB and HDAC2, which are both nuclear proteins, western blot analysis shows more protein in the nuclear extraction samples compared to the homogenate samples, with CREB showing higher levels of protein for the control sample but HDAC2 showing more protein in the *Rest* cKO. For the immediate early gene *Arc*, a similar pattern can be seen. More protein can be seen in the nuclear extraction samples compared to the homogenate samples and levels of protein seem higher in the *Rest* cKO compared to the control. However, when observing the western blot for the immediate early gene *Npas4*, more protein is seen in the homogenate samples rather than the nuclear extraction samples. With more protein seen in the control sample rather than the *Rest* cKO. The data commented above can be seen in **figure 5b** using the normalised quantification values.

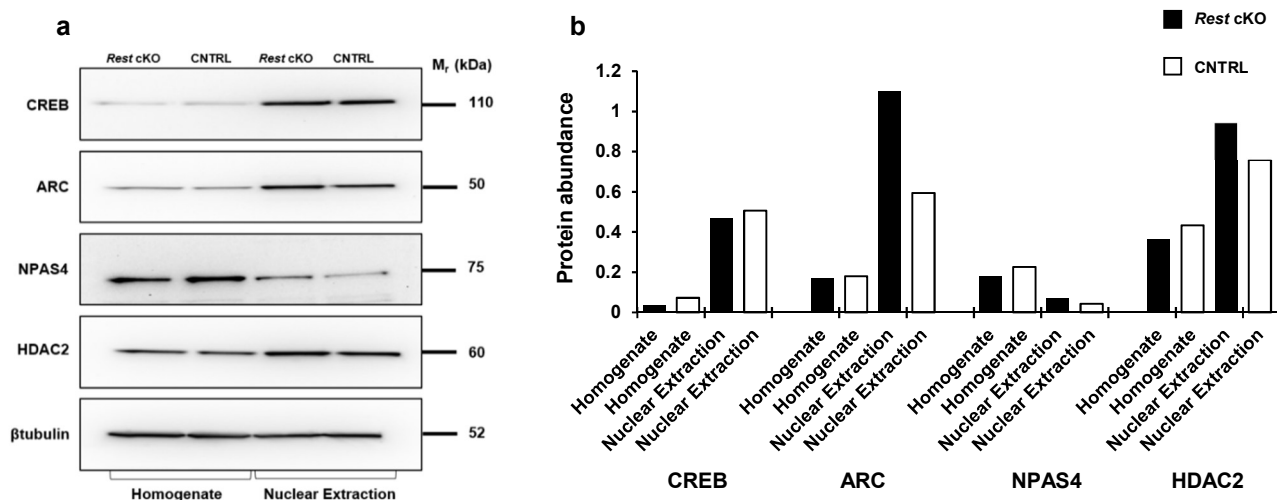


Figure 5

An increase in ARC, NPAS4 and HDAC2 protein in *Rest* cKO in nuclear fractions but a decrease in CREB

Western blot comparison of cortex homogenate and nuclear extraction. 10 μ g of homogenate and nuclear extraction sample was used for all blots, this was controlled for as data was normalised against the loading control (β tubulin). **a**, shows the western blot images with CREB bands imaged at 110kDa, ARC at 50kDa, NPAS4 at 75kDa, HDAC2 at 60kDa and the loading control β tubulin at 52kDa. **b**, shows the corresponding graph for all antibodies against the protein abundance after normalisation with the loading control. For each antibody, the graph presents the homogenate and nuclear extraction samples for both the *Rest* cKO sample and the control. Values represent the mean \pm range, ($n=2$).

3.6 ARC

Samples were prepared from the neocortex and the hippocampus, to evaluate if there was a difference in the amount of protein between the two regions and, between the controls and *Rest* cKO in homogenate and nuclear extraction samples. **Figure 5** does not show a significant difference between the homogenate samples and the nuclear extraction samples, but generally more protein is seen in the *Rest* cKO samples in the cortex but less in the hippocampus. Overall more protein is observed in the neocortex compared to the hippocampus, although this is also seen in the loading controls for both homogenate and nuclear extraction as seen in **figure 6a** and **6b**. When observing the nuclear extraction cortical samples in **figure 6c**, more protein is seen in the control samples compared to the *Rest* cKO.

A t-test was run on the data observed in **figure 6c**, in order to see if there is a significant difference in the amount of protein observed between control samples and *Rest* cKO when using anti-ARC. The t-test showed that there was not a significant difference in protein levels between control samples and *Rest* cKO ($p = .23$).

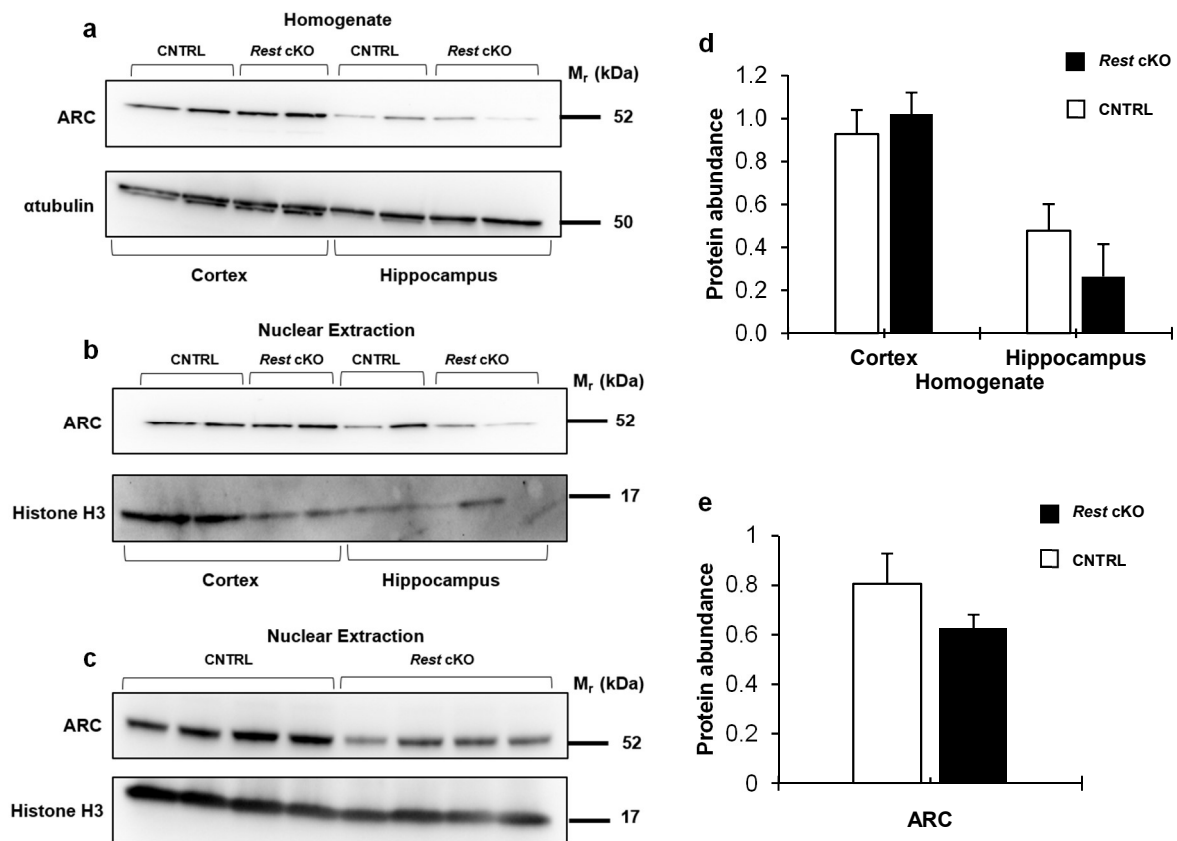


Figure 6

Increase in ARC protein for *Rest cKO* mice in the cortical homogenate samples but a decrease in cortical nuclear fractions

Western blot comparison of homogenate and nuclear extraction samples in the cortex and hippocampus for **a** and **b**, but only cortical samples in **c**. ARC protein bands were observed at 52 kDa. **a**, shows all homogenate samples from both genotype in the cortex and hippocampus. **b**, shows nuclear extraction samples which were used similarly for both the cortex and hippocampus, when comparing the two genotypes. **c**, shows only nuclear extraction samples in the cortex for *Rest cKO* and controls. **d**, represents the quantified values for the homogenate samples seen in **a**. Values represent the mean \pm range, ($n=2$). **e**, represents the quantified values for the nuclear extraction samples seen in **c**. Values represent the mean \pm s.e.m, ($n=4$).

3.7 HDAC2

Analysis of western blots show more HDAC2 protein in the cortex than the hippocampus for homogenate samples, with *Rest* cKO having slightly more protein. For the hippocampal homogenate samples in **figure 7a**, the control samples seem to have more HDAC2 protein than the *Rest* cKO. When evaluating the western blot images for the nuclear extraction in **figure 7b**, *Rest* cKO samples seem to have more HDAC2 protein in the cortex however, they seem to have less protein in the hippocampus.

When analysing **figure 7e** and **7f**, for the homogenate samples, more protein can be seen in the *Rest* cKO compared to the controls. However, for the nuclear extraction samples more protein can be seen in the controls compared to the *Rest* cKO samples. The difference in the density of the bands between the homogenate and nuclear extraction blots could be due to the change in exposure time. Even though the optimal exposure time was optimised, slight changes were seen in the exposure time across different blots.

For **figure 7e** and **7f**, as there are 4 samples of each genotype a t-test was run in order to analyse if there is a significant difference in the level of protein between *Rest* cKO and control samples. The t-test showed that there was no significant difference between *Rest* cKO and controls in the homogenate samples ($p= 0.07$) or the nuclear extraction samples ($p= 0.13$).

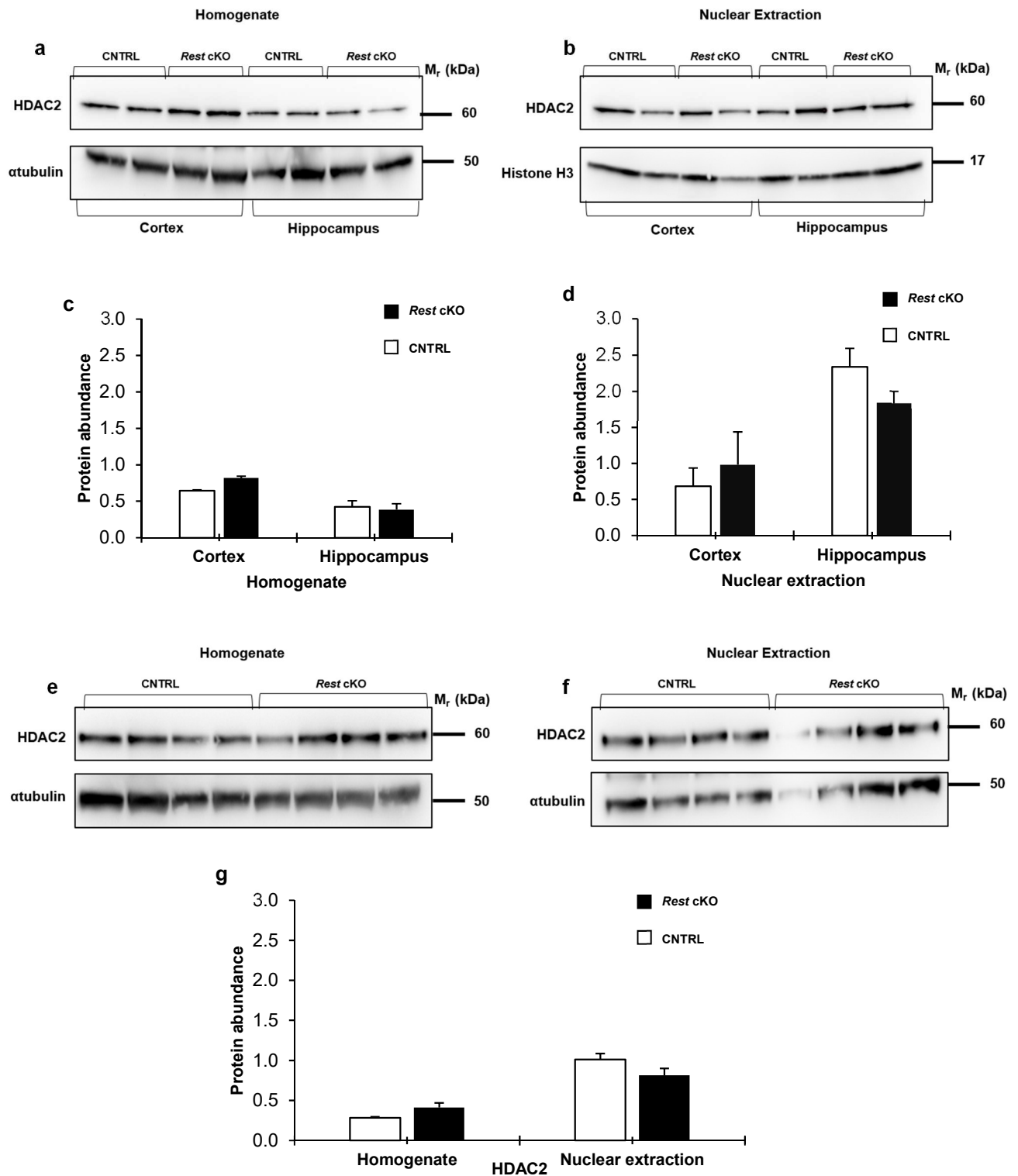


Figure 7

An increase in HDAC2 protein in the cortex of Rest cKO

The images involve the corresponding western blot data and graphs obtained following quantification. HDAC2 protein bands were imaged at 60kDa. **a**, shows all homogenate samples when comparing between the cortex and hippocampus. **b**, shows all nuclear extraction samples when comparing between the cortex and hippocampus. **c**, represents the quantified values from the homogenate samples seen in **a**. Values represent the mean \pm range, ($n=2$) **d**, represents the quantified values from the nuclear extraction samples seen in **b**. Values represent the mean \pm range, ($n=2$). **e**, shows all homogenate samples comparing controls and Rest cKO. **f**, shows all nuclear extraction samples comparing controls and Rest cKO. **g**, represents the quantified values from homogenate samples in **e** and nuclear extraction samples in **f**. Values represent the mean \pm s.e.m, ($n=4$).

3.8 CREB

Western blot CREB protein analysis of both neocortex and hippocampal shows varied findings. For the homogenate samples, more protein is seen in the cortex than the hippocampus, this could have been due to an error when loading the samples as suggested by the loading control. When data was quantified for **figure 8a**, negative values were obtained either due to the faintness of the bands or high background. Thus, these values are not included in **figure 8**. Focusing on the nuclear extraction samples, more protein is seen in the hippocampal samples when compared to the neocortex, with more protein being present in the controls compared to the *Rest* cKO. Despite this, the error bar seems to suggest there is a lot of variability.

When analysing **figure 8c**, more protein is seen in the *Rest* cKO compared to the controls. The same pattern is seen when analysing the nuclear extraction in **figure 8d**, although the difference between *Rest* cKO and controls is not as clear. As more protein is not seen across all western blots in *Rest* cKO samples, the findings do not give a clear conclusion.

For **figure 8c** and **8d**, due to there being 4 samples of each genotype on each western blot a t-test was run in order to see if there was a significant difference between the two genotypes in both homogenate samples and nuclear extraction samples. The t-test showed no significant difference between controls and *Rest* cKO in the homogenate samples ($p = .38$) or the nuclear extraction samples ($p = .77$).

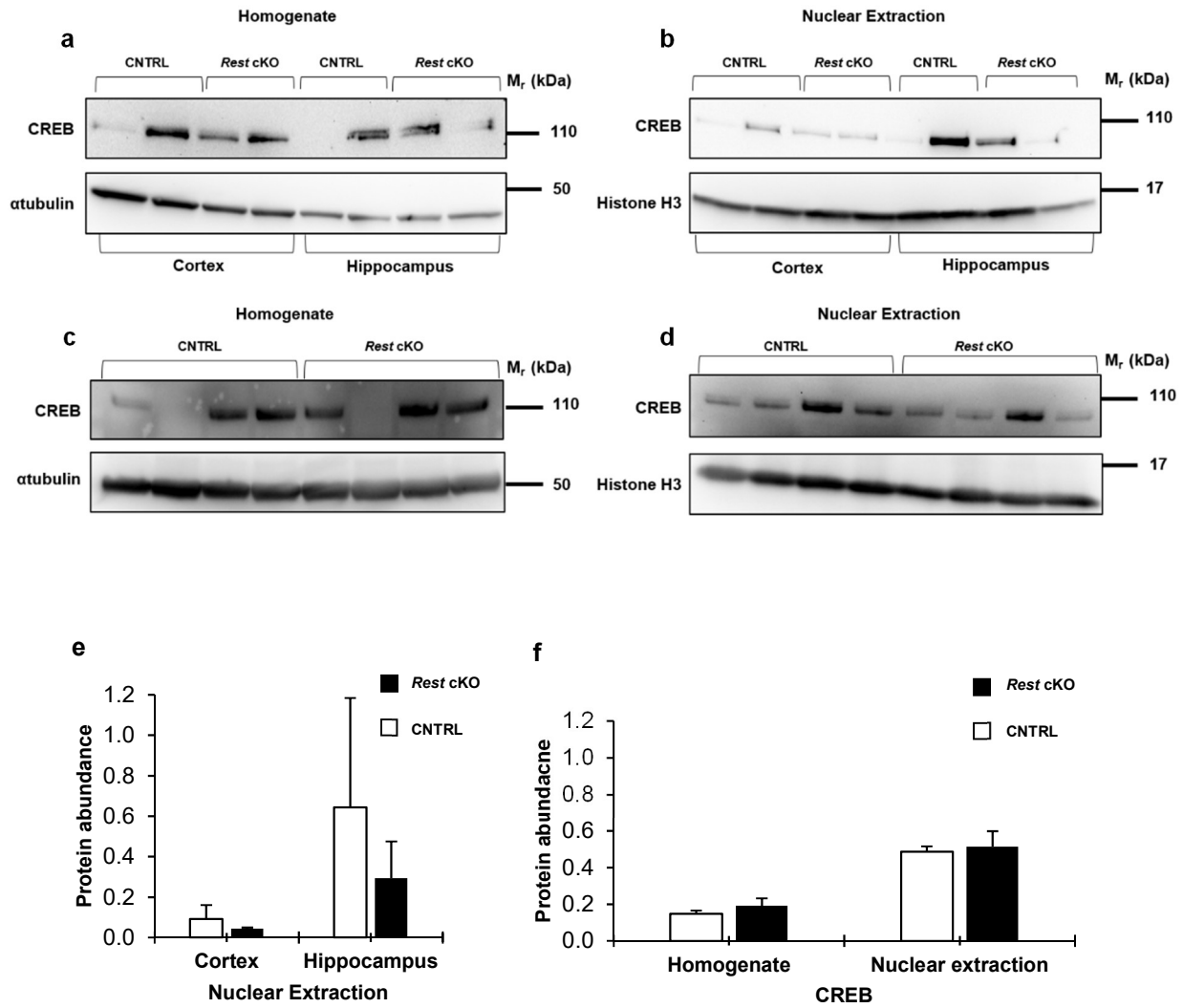


Figure 8

No difference in CREB protein expression between *Rest cKO* and controls in the cortex or hippocampus

Western blot data imaged above shows CREB protein bands are imaged at 110kDa. **a**, homogenate samples from both genotypes in the cortex and hippocampus. **b**, nuclear extraction samples from both genotypes in the cortex and hippocampus. **c**, homogenate samples from the cortex only. **d**, nuclear extraction samples from the cortex only. **e**, represents the quantified values for samples in **b**. Values represent the mean \pm range, ($n=2$) **f**, represents the quantified values for the homogenate samples in **c** and the nuclear extraction samples in **d**. Values represent the mean \pm s.e.m, ($n=4$).

3.9 Phosphorylated CREB (Ser133)

The phosphorylated CREB antibody used in this study is designed to detect endogenous levels of CREB when phosphorylated at serine 133. Cortical tissue only was used when investigating phosphorylated CREB. Western blot analysis showed 2 bands at 250kDa and 70kDa. When observing **figure 9**, bands are seen in the nuclear extraction samples but not in the homogenate for both genotypes, as phosphorylated CREB is a nuclear protein. The bands seem to be stronger in the controls suggesting more phosphorylated protein than in the *Rest* cKO. The company from which the antibody was obtained (see 2.18 antibodies), suggest that bands should be visualised at a molecular weight of 43kDa. As no bands appeared at this molecular weight it is appropriate to suggest that the correct bands are either at 250kDa or at 70kDa. The predicted band size which is thought to appear at 43kDa may be a product of a different type of sample such as cell culture rather than brain tissue which could possibly explain this observation. No form of quantification was undertaken on the western blots due to the high background signal observed.

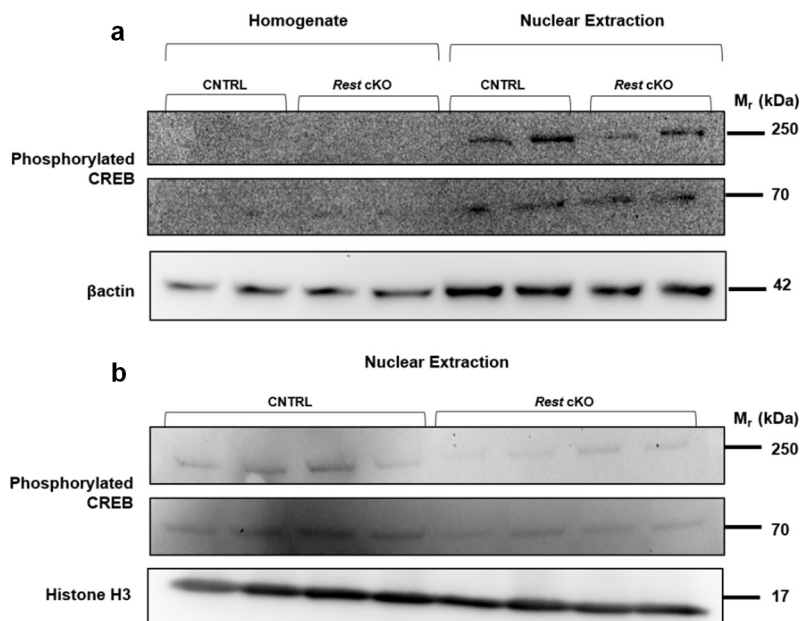


Figure 9

A reduction in the levels of phosphorylated CREB protein observed in the *Rest* cKO samples

Analysis of western blot data following the use of phosphorylated CREB show stronger bands in the control genotype. **a**, involves the comparison of control and *Rest* cKO for homogenate samples and nuclear extraction samples. **b**, shows comparison of controls and *Rest* cKO in nuclear extraction samples. β actin was used as the loading control for **a** due to there being homogenate samples. For the nuclear extraction samples the nuclear loading control Histone H3 was used. Bands for both blots are seen at 250kDa and at 70kDa.

3.10 NPAS4

As well as comparing between control samples and *Rest* cKO, this study wanted to confirm whether there were any differences between the cortical homogenate and the nuclear fractions. Analysis of data when using NPAS4 suggests more protein in the *Rest* cKO genotype compared to controls in both the homogenate and the nuclear fractions. When observing the western blot for the homogenate fractions, there seems to be a greater difference between the control and the *Rest* cKO samples, with more protein being seen in the *Rest* cKO, as seen in **figure 10c**. Another point which must be made is that NPAS4 is a nuclear protein, thus it should only be seen in the nuclear fractions. However, bands of a similar density are seen in the homogenate fractions. As the western blots in **figure 10a** and **10b**, were taken separately an explanation for the similar density of bands between the two could be the exposure time. **Figure 10a**, could have had a longer exposure than **10b**, which would explain this.

As 4 samples per genotype were used in both western blots t-tests were run to confirm whether this result was significant. The t-tests suggested that there was no significant difference between controls and *Rest* cKO in the homogenate fractions ($p = .23$) or the nuclear extraction fractions ($p = .69$).

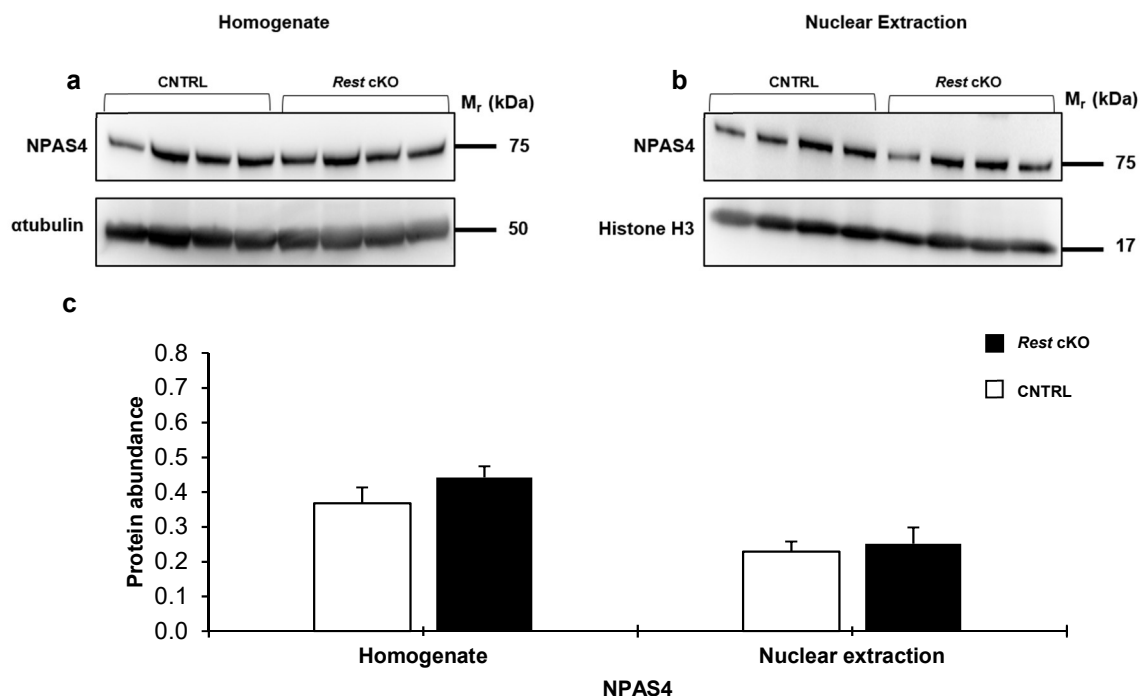


Figure 10

An increase in NPAS4 protein observed in the *Rest* cKO samples compared to control

Analysis of western blot data following the use of NPAS4 show stronger bands in *Rest* cKO. NPAS4 protein bands were observed at 75 kDa. **a**, involves the comparison of control and *Rest* cKO for homogenate samples **b**, shows comparison of controls and *Rest* cKO in nuclear extraction samples. actubulin was used as the loading control for **a** due to there being homogenate samples. For the nuclear extraction samples the nuclear loading control Histone H3 was used. **c**, represents the data quantified for both homogenate and nuclear extraction samples. Values represent the mean \pm s.e.m, ($n=4$).

3.11 C-FOS

Western blot analysis of C-FOS protein showed bands at multiple molecular weights, as seen in **figure 11**. Investigation as to which bands were at the correct molecular weight for C-FOS proved to be difficult as the antibody had only been used in cell culture and rarely in mouse brain. When focusing on **figure 11a**, it was originally assumed the correct band was at 150kDa, due to the bands being the strongest at this molecular weight, suggesting no difference in protein levels when comparing the *Rest* cKO and control. If the correct bands are one of 190, 100 or 75kDa, the result would be interesting as C-FOS is a nuclear protein although can only be seen in the homogenate samples. When focusing on **figure 11b**, the same problem arose, as in **figure 11a**. When analysing the band at 190kDa, the *Rest* cKO samples seem to have slightly more protein than the controls. Although the same result isn't seen for the last band. When observing the loading control more sample seems to be added to that sample which is suggestive of an interesting result. Focusing on the nuclear extraction western blot in **figure 11c**, the strongest band at 150kDa is most likely the correct band, though this isn't definitive. The band at 150kDa is suggestive that there is more protein in the *Rest* cKO samples when comparing to controls.

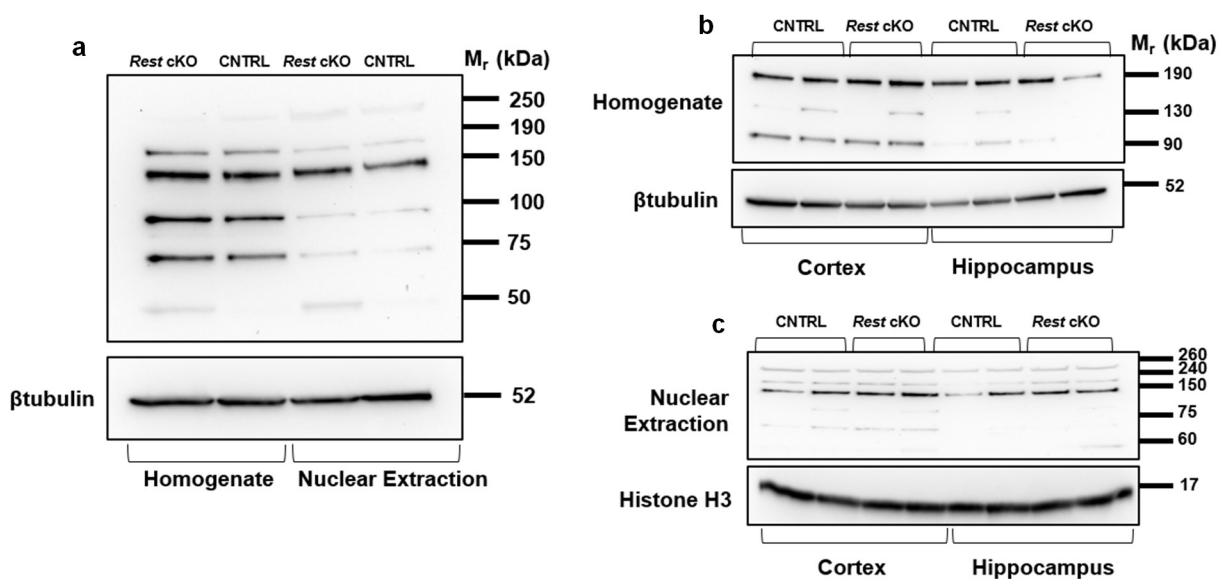


Figure 11

Multiple C-FOS protein bands observed in both homogenate and nuclear fractions

Western blot images shown for **a**, only the cortex for both homogenate and nuclear extraction samples and **b**, homogenate samples in both the cortex and hippocampus **c**, nuclear extraction samples in both the cortex and hippocampus. As it is not clear which bands are at the correct molecular weight, all have been shown.

3.12 EGR-1

Analysis of the western blot findings which explored EGR-1 protein levels showed multiple bands. Investigation of the appropriate molecular weight for EGR-1, showed to be around 75kDa. Despite changing the exposure time on several occasions, and the dilution of the antibody the bands never became strong enough to quantify at this molecular weight. When analysing **figure 12a**, all bands appear stronger in the homogenate samples compared to the nuclear extraction. When analysing **figure 12b**, more protein is observed in the *Rest* cKO samples compared to the controls, across all bands. The loading control, β tubulin, seems fairly even across all samples despite some small changes in protein loading, suggesting that this result is most likely not an artefact but rather a true representation of the amount of protein in *Rest* cKO samples. Focusing on **figure 12c**, more protein is seen in the cortex when compared to the hippocampus and it seems that bands appear stronger for the *Rest* cKO samples in the bands at 125kDa but also those at 110kDa.

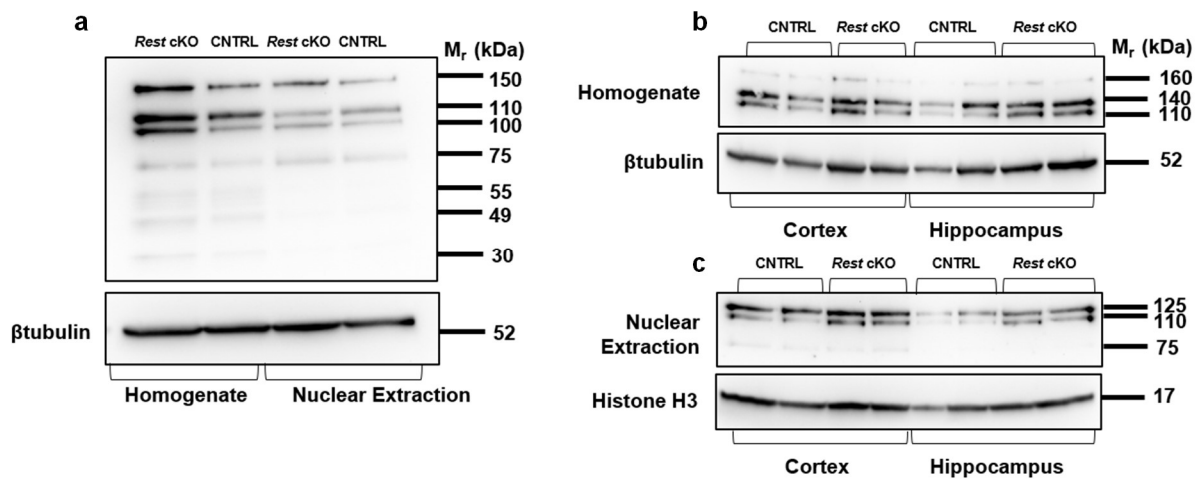


Figure 12

Multiple EGR-1 protein bands observed in both homogenate and nuclear fractions

Western blot images shown for **a**, only cortical samples for both homogenate and nuclear extraction was used. **b**, homogenate samples for the cortex and hippocampus with β tubulin as the loading control. **c**, the nuclear extraction western blot is seen comparing *Rest* cKO samples to controls in both the cortex and hippocampus, using histone H3 as the nuclear loading control. As it is not clear which bands are at the correct molecular weight, all have been shown.

4.0 Immunohistochemical analysis

Immunohistochemistry was undertaken using the antibodies against the following proteins: **NeuN**, **GFAP**, **Synaptophysin** and **MAP2**, to determine if any differences are seen between *Rest* cKO and control samples. The two brains of each pair were sectioned the same day and the sections from them were always processed together. Prior to conclusions being drawn, all *Rest* cKO samples were matched with their control pair following histology using haematoxylin and Nissl staining. Sections were observed using the microscope (see 2.15 image acquisition) before being matched using the mouse brain atlas (Franklin and Paxinos, 2019) in terms of sagittal plane. Quantification for most samples was undertaken blindly by 3 students in which an average was calculated based on these values.

4.1 NeuN

The neuronal nuclear protein, NeuN, is used as a marker for neurons. Standard immunohistochemistry protocol was followed with the addition of citrate antigen retrieval. Using the citrate antigen retrieval helps to greatly improve detection of some proteins. The protocol was followed for 3 pairs of mice. When analysing **figure 13**, no clear differences can be seen between the pairs of mice or within each pair. However, when observing pair 1, the hippocampus for the *Rest* cKO seems to appear more neuronally dense than the control.

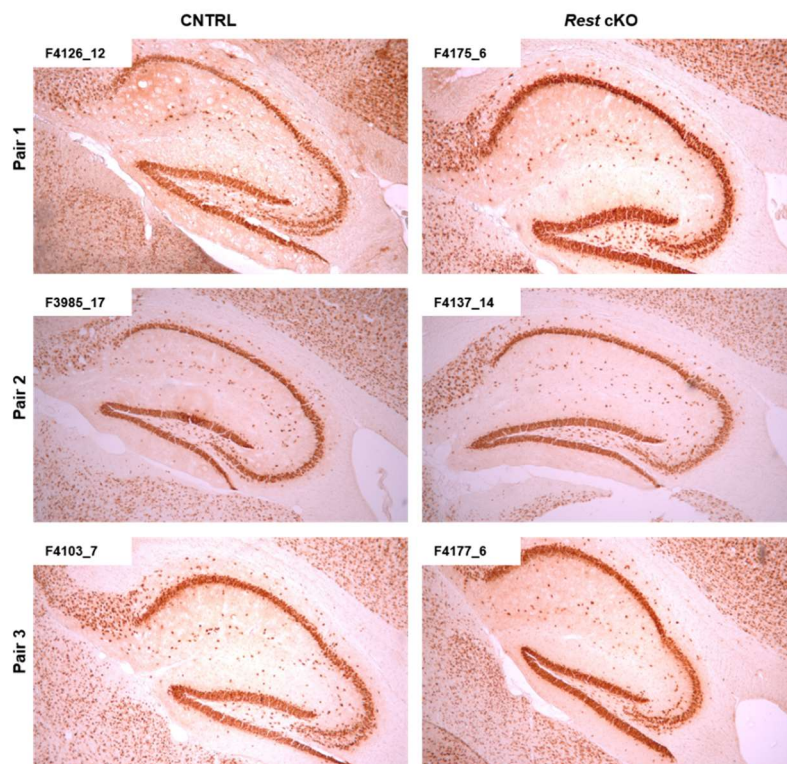


Figure 13

The hippocampus with NeuN staining

The whole hippocampus in 3 *REST* cKO mice and 3 controls was imaged using 5x magnification. Sections between each pair of mice were matched with regards to sagittal plane so comparison could be accurate.

Analysis of **figure 14** shows the different regions of the hippocampus being more neuronally dense in some *Rest* cKO samples compared to the controls. Specifically, the first *Rest* cKO sample in **figure 14a** looks more neuronally dense in the CA1 compared to its matched pair. No visible differences can be seen when analysing the second pair for the CA1. However, when focusing on the third pair the CA1 region for the *Rest* cKO mouse seems to be thicker when comparing to its matched control pair. When observing the CA3 and DG, the same can be seen between the pair on the first row, but not for the other two pairs of mice. Analysing the graph in **figure 14d**, shows the quantified values for all regions. More neuronal nuclei are seen in the *Rest* cKO in the CA1 and DG, but less in the CA3 compared to controls.

A (two-tailed) t-test was run using the quantification data obtained by counting the neuronal nuclei following the NeuN stain. The t-test suggested that there was no significant difference in neuronal nuclei between controls and *Rest* cKO samples in the CA1 ($p=.38$) or the CA3 ($p=.70$), however a significant difference was seen between controls and *Rest* cKO samples in the DG ($p<.05$) and in the total number of neuronal nuclei quantified across all regions of the hippocampus ($p<.01$).

As data was quantified for all regions of the hippocampus for all samples following NeuN IHC, an ANOVA was run. A one-way within subjects ANOVA showed that there was no significant difference in the pattern of neuronal nuclei between the CA1, CA3 or the DG of the hippocampus between *Rest* cKO and controls: $F(2,3)=1.843$, $p=.22$.

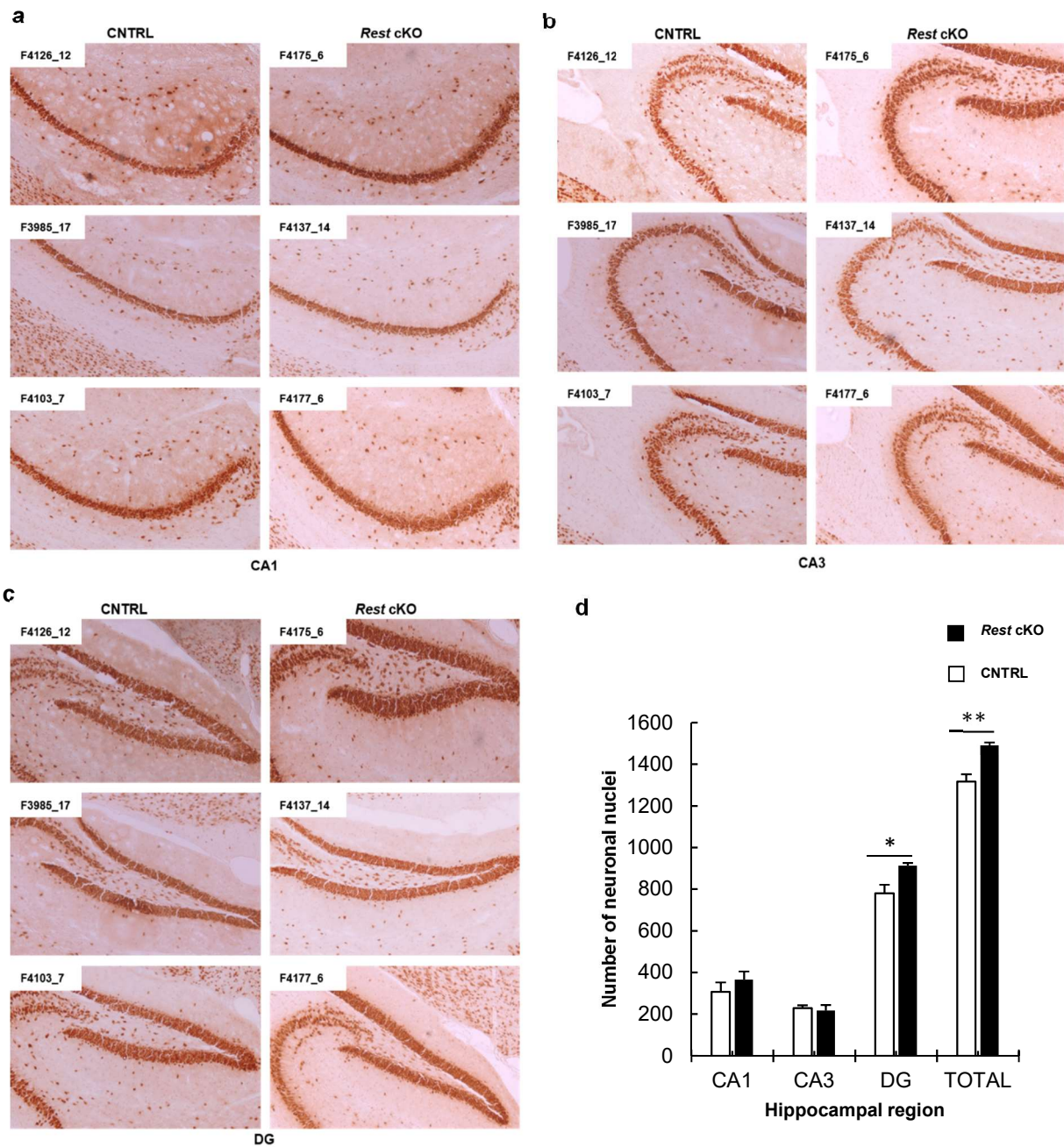


Figure 14

A greater number of neuronal nuclei observed in the CA1 and DG region of the hippocampus in *REST cKO*

The images above were taken at a magnification of 10x. This was undertaken after using NeuN IHC staining so the neuronal number could be determined between the different pairs of *Rest cKO* mice and controls. The images show for **a** the CA1, **b** the CA3 and **c** the dentate gyrus for each mouse. Medial sections were matched across all pairs of mice. **d**, represents the values following quantification of neuronal nuclei. Values represent the mean ± s.e.m. ($n=3$).

4.2 GFAP

GFAP was used as a marker of astrocytes, as activation of more astrocytes is suggestive of a neurodegenerative phenotype. **Figure 15** is used as a general representation of all mouse pairs. When analysing the control and *Rest* cKO images of the whole hippocampus in this section in **figure 15**, there seems to be more astrocytes localised around the pyramidal cell layer in the CA1 region of the hippocampus.

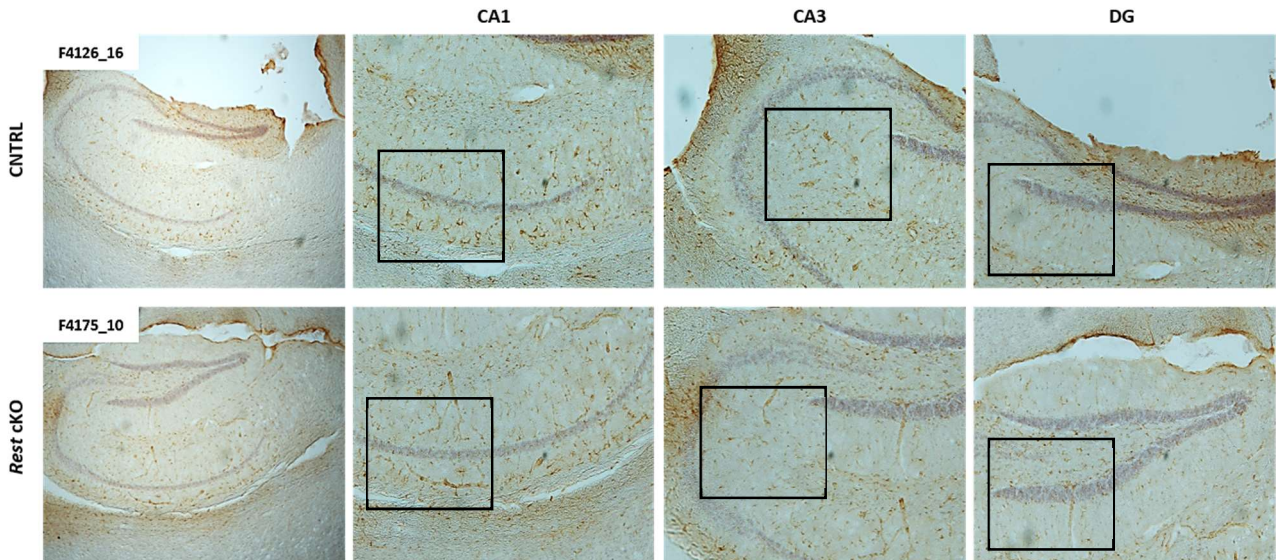


Figure 15

Astrocytes in *Rest* cKO and control samples in lateral sections of the hippocampus

The hippocampus was counterstained using haematoxylin for better visualisation. The first image for both the knockout and control was taken using 5x magnification, whereas, the later images showing the different regions of the hippocampus, the CA1, CA3 and DG were taken at 10x magnification.

When observing the CA1 in **figure 16a**, it appears there are more astrocytes in the control compared to the *Rest* cKO. However, imaged is just a small region of the CA1, as this finding may be accurate for that specific area of the CA1, by quantifying the whole CA1, more astrocytes are seen in the *Rest* cKO. When analysing the CA3 and DG in **figure 16a**, slightly more astrocytes can be seen in the control rather than the *Rest* cKO. In contrast to the CA1, this observational analysis is supported by quantitative data which seems to suggest the same is seen across the whole CA3 and DG not just that region imaged specifically. All images in **figure 16a** have staining of the hippocampus using haematoxylin.

A (two-tailed) t-test was run using the quantification data obtained by counting the astrocytes following the GFAP stain. The t-test suggested that there was no significant difference in neuronal nuclei between controls and *Rest* cKO samples in the CA1 ($p=.35$), the CA3 ($p=.88$), the DG ($p=.43$) or in the total number of astrocytes quantified across all regions of the hippocampus ($p=.74$).

As data were quantified for all regions of the hippocampus for all samples following GFAP IHC, an ANOVA was run. A one-way within subjects ANOVA showed that there was no significant difference in the pattern of astrocytes between the CA1, CA3 or DG of the hippocampus between *Rest* cKO and controls: $F(2,3)=1.566$, $p=.27$.

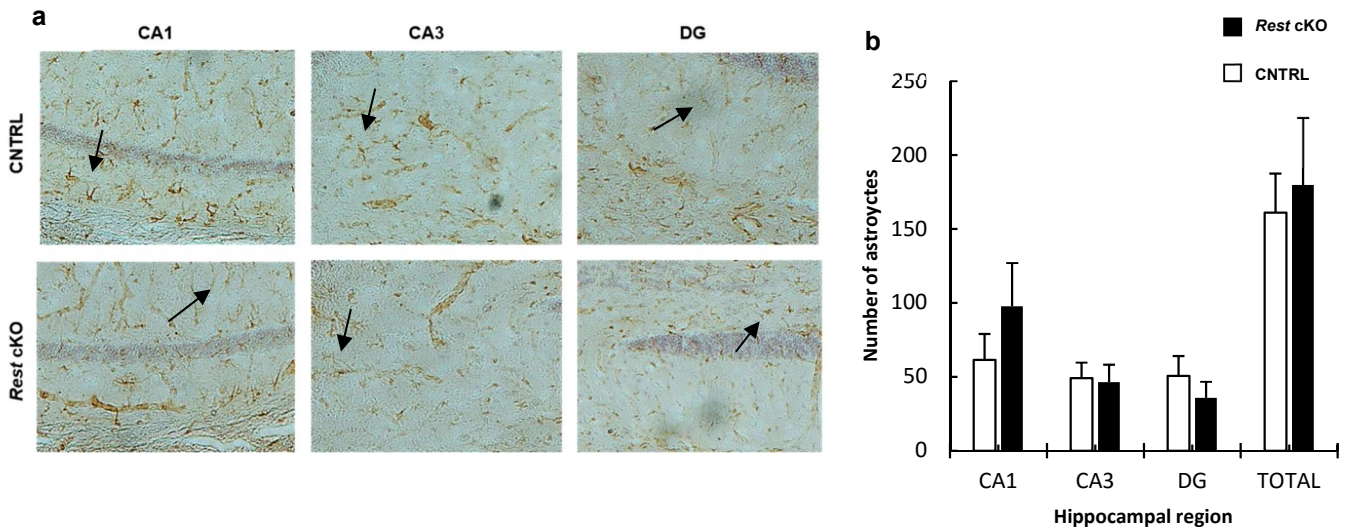


Figure 16

An increase in astrocytes in *Rest* cKO in the CA1

a, images taken at a magnification of 10x for the CA1, CA3 and DG of the representative pair of mice were further magnified. Arrows indicate astrocytes. **b**, the graph represents the values obtained from quantification, comparing the hippocampal region against the number of astrocytes in *Rest* cKO and controls. Values represent the mean \pm s.e.m. ($n=3$).

4.3 Synaptophysin

Synaptophysin was used as a marker for synapses. Specifically, to observe whether there are any differences in the synaptic terminals in *Rest* cKO and controls. Performing immunohistochemistry against synaptophysin showed that the staining had worked due to the brown colour seen in **figure 17**, however it was difficult to observe the synaptic terminals down the microscope and the 20x magnification images taken. Thus, no form of quantification could be undertaken.

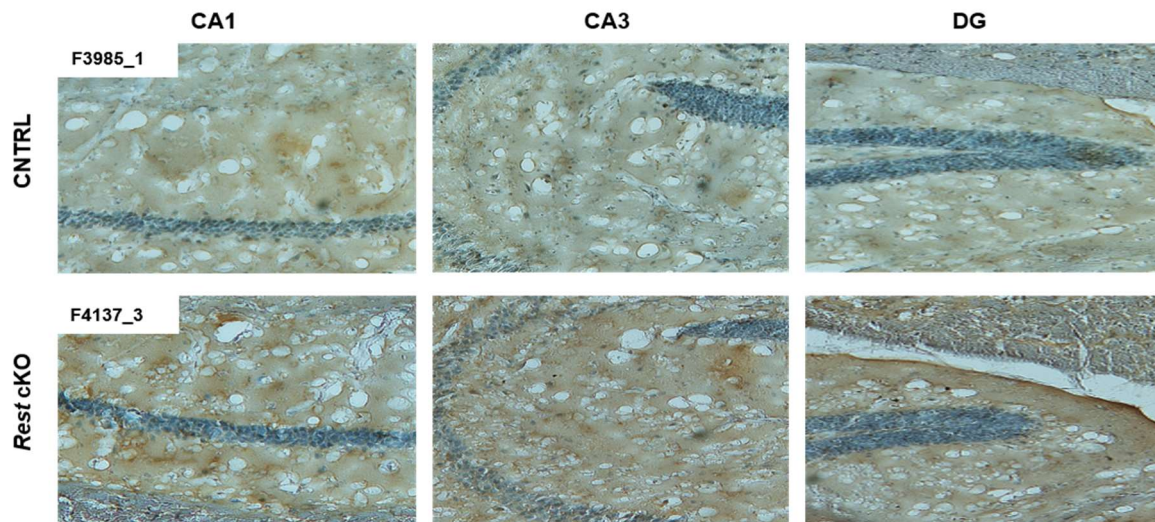


Figure 17

Using synaptophysin as a marker of synapses proved to difficult for analysis

Images seen were used as representatives for the two genotypes. The images for the CA1, CA3 and DG for the sample pair were initially taken at 10x magnification. Shown are the further magnified images.

4.4 MAP2

MAP2 was used as a dendritic marker. Dendrites were seen across all samples, of both *Rest* cKO and controls. Due to the quantity of dendrites, quantification was difficult, therefore assumptions were made on which genotype had a greater number of dendrites. **Figure 18a** is a representative image of a pair of samples.

Focusing more on the different regions of the hippocampus, areas of the CA1, CA3 and DG in the representative pair have been enlarged to show the dendrites and to see if there is a visible difference in the number of dendrites between the *Rest* cKO and control. Based on observation, when analysing **figure 18b**, more dendrites can be seen in the control compared to the *Rest* cKO, in all regions of the hippocampus studied below.

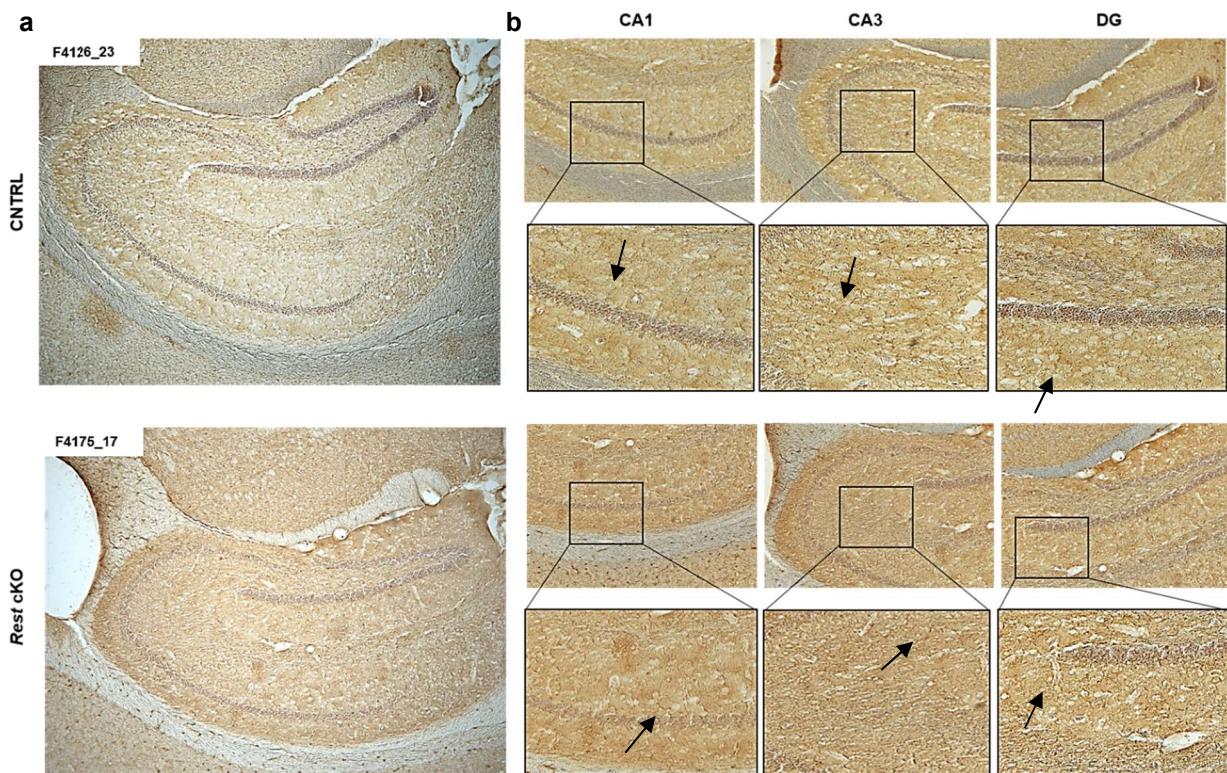


Figure 18

Using MAP2 as a marker of dendrites

a, The whole hippocampus was imaged at a magnification of 5x following IHC against MAP2. b, The images for the CA1, CA3 and DG for the sample pair were taken at 10x magnification. These images were further magnified to be able to better see the dendrites. Arrows indicate dendrites.

MAP2 analysis involved comparing the dendrites between *Rest* cKO and controls by comparing the length, structure, direction and other dendritic properties. This analysis was carried out by 3 students and was based on observation alone.

Table 2

Table showing the properties analysed in dendrites in *Rest* cKO and controls

Comparison of dendrites between 3 pairs of mice ($n=6$), the different regions of the hippocampus were studied separately in order to draw a more accurate conclusion. The length and quantity of the dendrites was determined by observation and noted, as well as the orientation and specific location.

	Genotype	Region	Length	Quantity	Orientation	Localisation
Pair 1	CNTRL	CA1	Short	Less	No common direction	Scattered
		CA3	Long	More	No direction	Scattered
		DG	Long	More	Well defined	Scattered
	<i>Rest</i> cKO	CA1	Long	More	Pointing towards the DG	More between CA1 and DG
		CA3	Short	Less (medial); more (lateral)	Pointing towards the medial region of the hippocampus	Scattered, more outside
		DG	Short	Less	Not well defined	Scattered
Pair 2	CNTRL	CA1	Long	Less but well defined	All seems to follow the same direction, more organised	More between CA1 and DG
		CA3	n/a	More defined	No common direction	Mostly inside of the CA3, some outside (other side of the cell bodies)
		DG	n/a	Less defined	No common direction	Between the dendritic borders
	<i>Rest</i> cKO	CA1	Short	Has more shorter dendrites	No common direction	Scattered
		CA3	n/a	Less defined	From CA3 to inside of the hippocampus	Inside of the CA3
		DG	n/a	More defined	No common direction	Between the dendritic borders
Pair 3	CNTRL	CA1	Long	More	No common direction	Scattered, more between the CA1 and DG
		CA3	Long	More	All seems to follow the same direction, more organised (outer hippocampus)	Has more dendrites outer hippocampus the CA3
		DG	Short	Very similar	No common direction	Between the dendritic borders
	<i>Rest</i> cKO	CA1	Short	Less	All pointing vertically	Scattered, more between the CA1 and DG
		CA3	Short	Less	No common direction	Closer to the pyramidal cell layer
		DG	Short	Very similar	No common direction	Between the dendritic borders

Concluding on the findings in **table 2**, the control samples seemed to have more dendrites which were longer in length but did not seem to follow a common direction, with a few exceptions. As such, the control in pair 1 for the CA1 and the control in pair 3 for the DG. The dendrites for the controls were generally scattered. Regarding the *Rest* cKO they seemed to possess less dendrites which were much shorter and were well localised to the region of the hippocampus analysed. In terms of the orientation for the dendrites in *Rest* cKO they commonly followed no common direction or were vertical.

5.0 Experiments on social memory related mechanisms

Previous behavioural work has suggested that the CA2 plays a role in social memory (Hitti and Siegelbaum, 2014). Western blotting and immunohistochemistry were undertaken, focusing on the cortex and hippocampus to see if there is a dysregulation in proteins or hippocampal structure, which could possibly explain social memory impairment.

5.1 Vasopressin V1B receptor

A western blot was performed to observe the V1BR protein levels between *Rest* cKO mice and controls. When analysing the neocortex, *Rest* cKO samples seem to have slightly more protein even though the loading control shows less protein was loaded in these lanes. However, the hippocampal samples suggest that when more protein is loaded for the *Rest* cKO mice, stronger bands are seen in the control samples, which is suggestive that the control samples have more V1B protein than the *Rest* cKO. The findings observed from the western blot in **figure 19a**, are presented in graph **19c**. Regarding the second western blot **19b**, the values obtained were paired with the cortex samples from **19a**, this was so statistical analysis could be undertaken. The t-test showed no significant difference in the amount of protein between controls and *Rest* cKO samples ($p = .31$). The values obtained following quantification were then calculated as a percentage using the controls, this can be seen in graph **19d**.

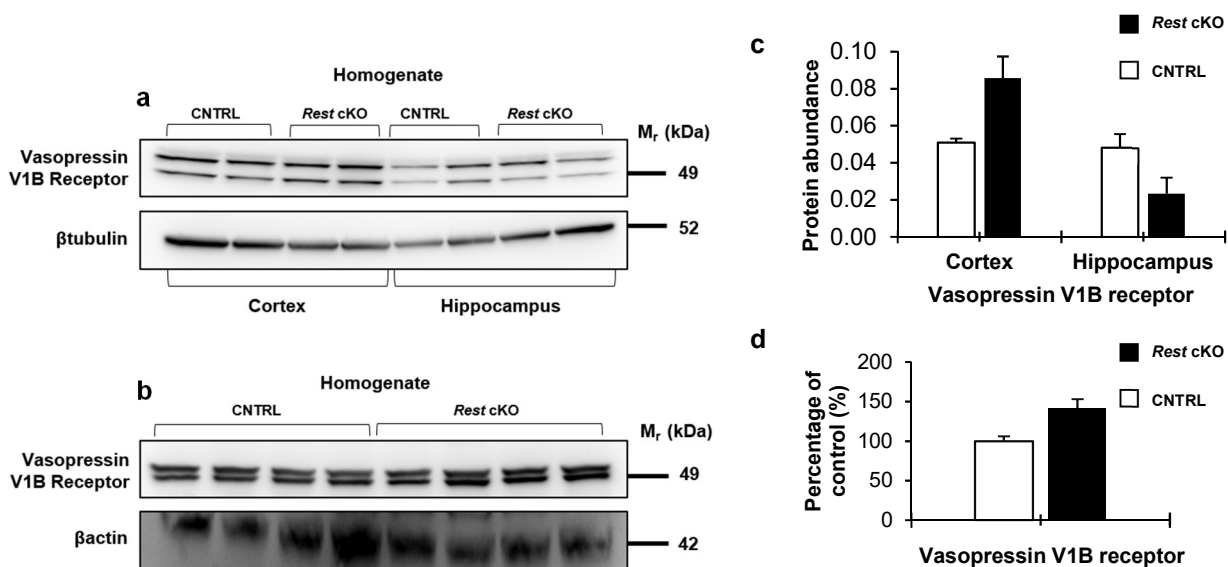


Figure 19

An increase in V1BR protein in the *Rest* cKO samples in the cortex

Western blot images shown for **a**, homogenate samples for both genotypes in the cortex and hippocampus. **b**, homogenate samples in the cortex only for both genotypes. **c**, represents the quantified values for homogenate samples seen in **a**. Values represent the mean \pm range, ($n=2$). **d**, represents the quantified values using the homogenate samples in blot **b**, and the cortex samples used in blot **a** as the graph demonstrates at what percentage the protein in the *Rest* cKO samples is greater than in controls. Values represent the mean \pm s.e.m, ($n=6$).

5.2 Oxytocin receptor

When observing the western blot, more oxytocin protein is seen in the *Rest* cKO compared to control samples. Though, this result isn't seen across all *Rest* cKO samples which makes the findings unclear. When observing the loading control β actin in **figure 20a**, there seems to be more sample in the last two lanes, suggesting the result seen may not be an accurate finding but rather a stronger band because of a greater quantity of protein. Due to no clear bands being visualised, quantification was unable to be undertaken.

5.3 Corticotrophin releasing factor (CRF)

By analysing **figure 20a**, the control samples seem to have more CRF protein when compared to the *Rest* cKO samples. The findings observed from the western blot are concluded in the graph in **figure 20b**. Due to there being 4 samples per genotype a t-test was undertaken to analyse whether the finding obtained was significant. The t-test showed that there was no significant difference in amount of protein between the controls and *Rest* cKO samples ($p = .17$).

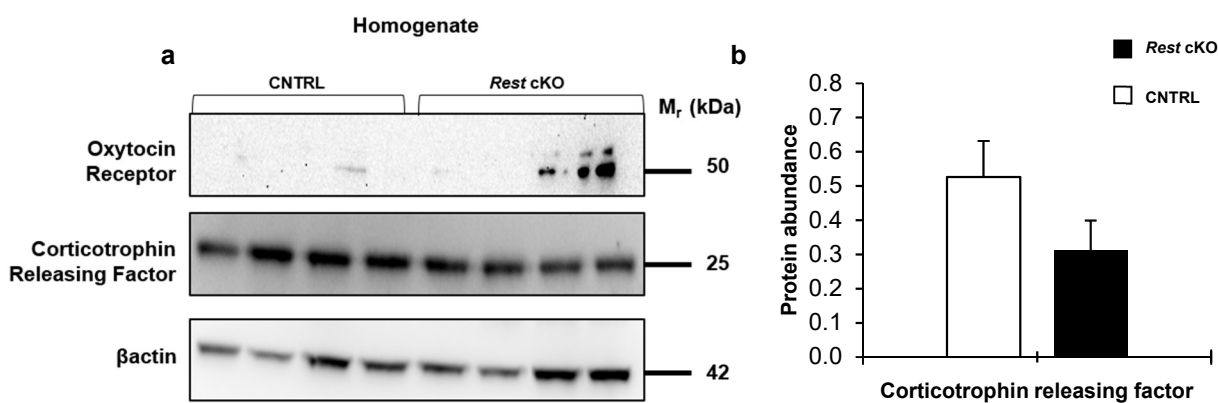


Figure 20

Higher levels of oxytocin receptor in *Rest* cKO but lower levels of CRF

Western blot findings shown for **a**, the oxytocin receptor in homogenate samples in the cortex, imaged at 50kDa and corticotrophin releasing factor (CRF) for homogenate samples in the cortex, imaged at 25 kDa. **b**, represents quantified values for the CRF western blot. Values represent the mean \pm s.e.m, ($n=4$).

5.4 Identifying area CA2

As well as investigating the protein abundance between *Rest* cKO samples and controls, the CA2 was identified following IHC using NeuN, which stains the neuronal nuclei. This was done by using the atlas and matching the sagittal planes of different sections to those referenced in the atlas. By doing this, identification of the CA2 became easier as certain characteristics became apparent such as small peaks in the pyramidal cell layer, allowing the CA2 to be distinguished from the CA1 and CA3. The CA2 was identified in all 3 pairs of mice. Borders were drawn onto the images to make quantification easier and to clearly demonstrate the CA2 region.

A (two-tailed) t-test was run using quantification data obtained for the CA2. 2 sections per mouse were quantified in which an average was calculated and used for the statistical analysis. The t-test was run in order to compare the number of neurons in the CA2 between *Rest* cKO samples and controls. The t-test showed that there was no significant difference when comparing the neurons in the CA2 between *Rest* cKO and controls ($p=.75$) Data is shown in **figure 21b**.

Figure 21c shows average values from pairs 1 and 3, disregarding pair 2 due to the gaps seen within the hippocampal tissue, specifically in the pyramidal cell layer of the hippocampus. The graph demonstrates a stronger difference between control and *Rest* cKO samples.

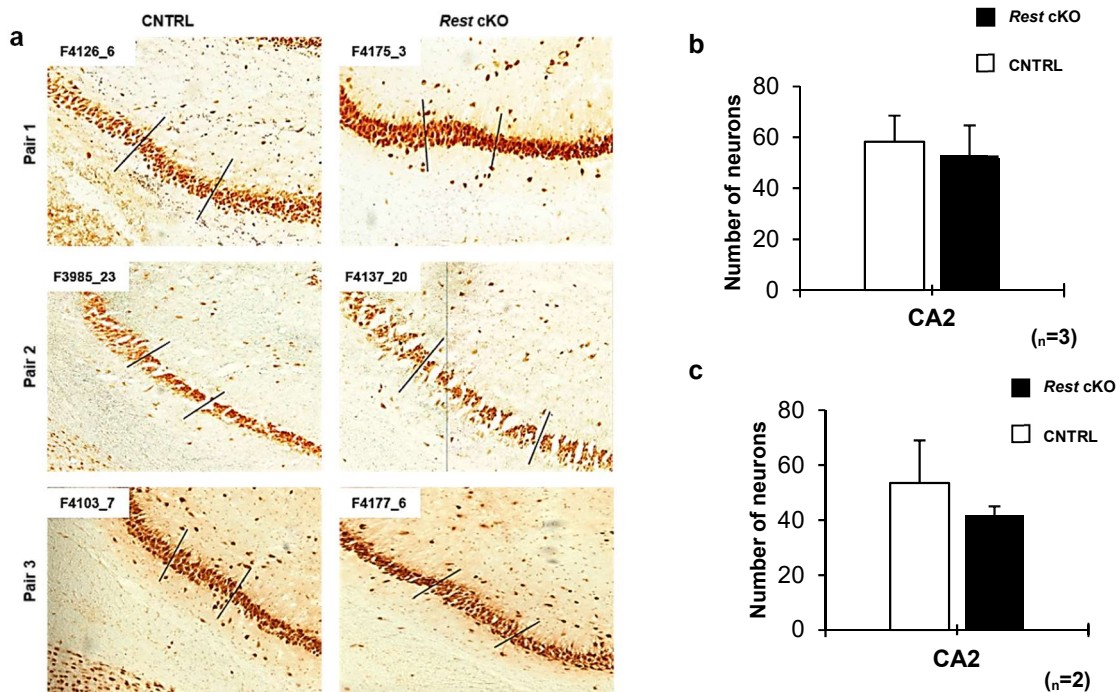


Figure 21

Identification of the CA2 on NeuN IHC sections

a, images obtained using the microscope at a magnification of 10x of the CA2 region. The marked borders clearly show the CA2, which was used for the quantification. **b**, the graph represents the quantification of the CA2 for all 3 pairs of mice. Values represent the mean \pm s.e.m ($n=3$). **c**, the graph represents quantification values obtained from pair 1 and pair 3, disregarding pair 2. Values represent the mean \pm range ($n=2$).

6.0 Discussion

Given the previous literature showing the importance of REST regulation for neuronal survival, this study aimed to further investigate the possible role of REST in neurodegeneration, through completion of western blot experiments, immunohistochemistry and histology. Using these experiments, the consequences of REST inactivation could be explored, with regards to expression of protein and brain morphology. The findings of this study suggest reduced levels of HDAC2 and phosphorylated CREB in *Rest* cKO samples compared to controls. Furthermore, a non-significant difference was seen in the quantity of activated astrocytes in the CA1 region of the hippocampus in *Rest* cKO mice. Analysis of additional morphological features showed a non-significant trend of less dendrites which were shorter in length in *Rest* cKO samples. When aiming focus on only the CA2 region of the hippocampus, findings suggest fewer neuronal nuclei as well as a reduction in V1B receptor protein in hippocampal samples in the *Rest* cKO mice.

In relation to the western blot experiments, findings from the present study showed that the IEGs which were mostly nuclear proteins, showed up stronger or only in the nuclear fractions and not in the homogenate. Previous studies propose that a reduction in IEGs suggests memory impairment (Palop *et al.*, 2003; Qiu *et al.*, 2016). Thus, when analysing the amount of protein in different IEGs and REST-related transcription factors the following non-significant trends were observed in the level of proteins: i) there was more ARC protein in the hippocampus of control samples than in the respective cortical homogenates; ii) more HDAC2 protein was seen in the *Rest* cKO in the cortex but less in the hippocampus in both the homogenate and nuclear fractions; iii) no clear interpretation of data was found when analysing CREB; iv) more phosphorylated CREB protein was seen in the cortical nuclear fractions of control samples; v) more NPAS4 protein was observed in *Rest* cKO in both homogenate and nuclear fractions of cortical samples. As briefly mentioned in the results section, analysis could not be undertaken for C-FOS and EGR-1, since multiple bands were seen at different molecular weights.

A few findings concerning ARC and NPAS4 support previous studies that suggest that IEGs are reduced during memory impairment (Rudinskiy *et al.*, 2012; Duran *et al.*, 2013). Regarding ARC, protein expression seemed to be non-significantly decreased in *Rest* cKO samples in the hippocampal homogenate samples and the cortical nuclear fractions. Similarly, the study by Palop *et al.*, (2005) suggests that *Arc* expression decreased but that this was located in the DG. The finding from the present study could be further explored to see if the same region is affected by undertaking IHC. However, in terms of NPAS4, as stronger levels of protein are seen in the *Rest* cKO samples in both homogenate and nuclear fractions it could be assumed that NPAS4 expression might be regulated by REST. This would suggest that the expression of NPAS4 is

inversely correlated with the expression of REST (Wu and Xie, 2006). Justifying this with regards to the present study, as REST is inactivated, higher levels of NPAS4 are observed.

A previous study demonstrates memory impairment when there was a reduced expression of HDAC2 (Guan *et al.*, 2009). Thus, given that REST is thought to be lost in AD or MCI, this would suggest that the levels of HDAC2 should similarly decrease. As the hippocampus is the major brain region responsible for memory, if there is HDAC2 more protein in control mice in the hippocampal samples compared to the *Rest* cKO, then the data obtained in this study correlates with the previous literature. The reason for the levels of protein in the *Rest* cKO being greater than in the controls in cortical samples is still unclear, though, it could possibly demonstrate that the neocortex does not play such a significant role in memory related behaviour as the hippocampus is known to do so. Though, this study did not focus on comparing protein expression in different brain regions and alternative experiments should be approached if this is to be evaluated. For example, using stereology to investigate the neuronal number between the two brain regions or through IHC, using an antibody against the protein in question to explore the distribution of these proteins. By undertaking analysis on HDAC2, it aids in understanding REST regulation with regards to memory.

Equally important, the data obtained for CREB produced findings which did not allow a conclusion to be made. When analysing the western blots, a few samples did not seem to show a protein band even though the loading control seemed equal across all samples. This was not committed in only one genotype. As CREB responds to many different stimuli, this variability in data could be due to other factors than the absence of REST. Since the mice were sacrificed, in a systematic manner and they were taken from the normal environment without any form of stimuli being present, these strong differences in the western blot data could be explained as a form of spontaneous behaviour.

Analysis of the data using phosphorylated CREB seemed to be the most promising. Previous studies suggest that the expression of phosphorylated CREB is lost when there is a memory deficit (Gong *et al.*, 2004; Barlotti *et al.*, 2016). As more protein was found in the control samples compared to the *Rest* cKO, the findings act as a catalyst in trying to explain memory impairment phenotypes but also in understanding the relationship between REST and CREB expression. Since REST was inactivated and there were lower levels of phosphorylated CREB protein, it suggests that REST dysregulation which leads to AD could happen via a dysfunction in the cellular mechanisms of CREB phosphorylation. Nonetheless, the findings obtained are preliminary and should be further explored by using more biological replicates enhancing the quantification of protein bands and allowing statistical analysis to confirm what has been observed. As CREB and phosphorylated CREB were used for analysis on the same samples,

figure 8d and **figure 9b** can be used to determine which molecular mechanism of the two transcription factors is responsible for the change seen in *Rest* cKO mice. When observing the quantified values of CREB in **figure 8f**, there is not a significant difference between the controls and *Rest* cKO. However, observing **figure 9b**, suggests there is more phosphorylated CREB protein in the controls. Overall, this proposes that there is a post-translation change in phosphorylated CREB expression in *Rest* cKO at Ser133, rather than a dysfunction in CREB gene expression.

For a few nuclear proteins, protein bands are seen in the homogenate samples and not in the nuclear fractions. This can be observed in **figure 5a** for NPAS4 but also in **figures 11** and **12**, for C-FOS and EGR-1. The definitive reason for this finding is unclear though there could be several explanations. Firstly, a problem may have occurred during the translocation of the protein to the nucleus from the cytoplasm. Correspondingly, some isoforms may be present in the homogenate samples which are recognised by the antibodies in question, although this does not explain how there is more protein in the homogenate and not in the nuclear extraction. Considering the possibility of cytoplasmic contamination in the nuclear fractions, it is evident that this is not the case. This is apparent as when other nuclear proteins were analysed, which were used on the same samples, they showed bands in only the nuclear fractions and not the homogenate. These findings determine the purity of the samples.

As multiple bands were seen in the western blots for C-FOS, EGR-1 and phosphorylated CREB, it is important to try and understand the reason for protein detection at several molecular weights. Possible explanations could be that the additional bands may be isoforms of the protein, the bands may be a cleaved product, or they may be due to unspecific binding. The best approach for this challenge in the future could be by acquiring a new antibody which is more specific, though this does not necessarily mean the same problem would not occur.

Concerning the western blot findings, the antibodies against phosphorylated CREB and *Npas4* were only used on cortical samples. The reason for this not being undertaken was greatly due to time restrictions. As REST was knocked out in the forebrain in excitatory neurons, where the hippocampus presents a greater percentage of these neurons when comparing to the cortex, it can be assumed that had the hippocampal samples been used the results could have been different. This should be investigated, as it could suggest a finding which has not been previously hypothesised but contributes to the understanding of some behavioural phenotypes.

NeuN was used to assess if there was a possible neurodegenerative phenotype. Although, the results found were not significant, they suggest more neuronal nuclei in *Rest* cKO mice in the whole hippocampus compared to controls. Taking the results into consideration, it can be concluded that no neurodegenerative phenotype was seen as there was no significant decrease in

neuronal number in *Rest* cKO mice. When focusing on the different regions of the hippocampus, the same finding was seen in the CA1 and DG but not in the CA3. This could suggest that the CA3 may be more selectively vulnerable, and that a neurodegenerative phenotype could first be seen in the CA3 rather than in any other hippocampal region. Another finding observed is that there were more neuronal nuclei in the *Rest* cKO mice in the DG. Possible hypotheses explaining this phenotype could involve an experimental problem. Also, another approach to understanding this could be that there may be significantly less neuronal nuclei in another section from the same sample. This suggests the importance of using multiple sagittal sections throughout the hemisphere for IHC to be able to draw representative conclusions. Another hypothesis to explain more neuronal nuclei seen in the *Rest* cKO samples in the DG could be through adult neurogenesis. As REST was conditionally knocked out after neuronal development, the deletion in REST could have initiated the production of more neurons via adult neurogenesis, due to the DG being 1 of 2 regions where adult neurogenesis takes place. However, this has already been previously explored in a study by Gao *et al.*, (2011) who suggest a reduction in neurogenesis in the DG. When establishing a link to the present study it proposes that the adult neurogenesis hypothesised could be an initial response, representing a brain repair system.

A similar pattern was observed when quantification was undertaken on astrocytes when comparing *Rest* cKO and controls. More astrocytes were seen in the control mice in the CA3 and DG regions but not in the CA1. It is unclear why there are many more astrocytes for the *Rest* cKO compared to controls in the CA1. Aiming to understand this finding, could be by examining GFAP as a marker of astrocytes and analysing its limitations. GFAP is seen as a sensitive marker that labels astrocytes (Sofroniew and Vinters, 2010). However, staining against GFAP for immunohistochemistry does not label all processes of the astrocyte just the key branches. As the quantity of astrocytes in this study was investigated rather than the structure of astrocytes, using this marker proved to be efficient. Furthermore, as microglia are activated earlier than astrocytes, and they promote astrocytic activation, a greater difference may be established between the genotypes when staining for microglia. This also may help to draw a conclusion as to why the CA1 seems vulnerable for activated astrocytes in *Rest* cKO mice.

Analysing dendritic properties was undertaken based on observation alone. Concluding on the findings seen in **table 2**, the control samples seemed to have more dendrites which were longer but did not seem to follow a common direction. Comparing those findings seen in the control samples, the *Rest* cKO seemed to possess less dendrites which were much shorter and did not seem as scattered. The findings are not completely congruent between the genotypes as well as the different regions of the hippocampus. In future, steps could be undertaken which allow quantification of dendrites either manually or through a software. This would allow statistical analysis to be performed giving the conclusions more strength. This would help when comparing

to previous literature by Gonzalez-Lima., (1998) which suggests when there is neurodegeneration there is a reduction in the apical dendrites in the CA1 region of the hippocampus. If the future recommendations are undertaken and there indeed proves to be a difference in dendrites in *Rest* cKO, it could suggest that there is not a loss of neurons but rather a loss of dendrites signifying dendritic degeneration.

As the supervisor has previously observed a repetitive memory impairment phenotype, this was further looked into and an additional region of the hippocampus, the CA2 was explored. When analysing the levels of V1BR protein, findings showed higher levels of V1BR protein in the hippocampal control samples compared to *Rest* cKO. When this finding was compared to that of previous literature, results seemed to show a similar conclusion. Chevalyere and Piskorowski (2016) demonstrated reduced social memory in V1BR knockout mice. Comparing the genotypes in cortical samples suggests an alternative finding, more protein was seen in the *Rest* cKO compared to controls. If the findings from the present study were repeated with more biological replicates it could possibly help with explaining memory impairment phenotypes and it could help with understanding the difference in V1BR protein levels in the neocortex and the hippocampus. Regarding the CA2 and the proteins analysed, IHC arises as a more useful alternative to study the distribution of proteins such as V1B in brain regions. This would allow better demonstration of the relationship between the protein and the CA2 region.

Aiming to explain the western blot results concerning the other two proteins of interest in social memory, previous studies suggest reductions in oxytocin and CRF are associated with memory impairment (Kasahara *et al.*, 2010; Lin *et al.*, 2017). The data obtained from this study shows high levels of oxytocin receptor in *Rest* cKO samples. This finding suggests there is no social memory impairment phenotype seen in the conditional knockout samples though, this finding cannot be used to draw conclusions. Firstly, the experiment was only undertaken once with 4 mice per genotype, but also, no clear bands were obtained in order to quantify using densitometry. This finding should be repeated to see if a replication in results is obtained prior to making any conclusions. The CRF western blot showed more protein in the control samples compared to the *Rest* cKO. This finding could be related to the previous study as a decrease in CRF expression is seen in both studies (Behan *et al.*, 1995), possibly suggesting cognitive impairment. However, conclusions cannot be drawn due to the small sample size used and the results were not replicated due to time restrictions.

Using cryostat sections which were stained with NeuN IHC and the mouse brain atlas, the CA2 was identified. The results seem to suggest that the controls had more neuronal nuclei compared to the *Rest* cKO mice. Even though statistical analysis was not undertaken as it was only possible to analyse 2 samples from each genotype, this should be repeated with more biological replicates

as it is possible that a significant value could be obtained, giving more strength to this hypothesis. With regards to the identification of the CA2 region, certain structural characteristics were identified which made this process more efficient and reliable. The second pair of mice were then disregarded due to having morphological holes as it would not give an accurate representative value of neuronal nuclei. These irregularities in the pyramidal cell layer could be due to several reasons not well understood.

Despite the promising findings observed in this study for the CA2 region of the hippocampus, further research is still necessary to elaborate on the possible role of REST in affecting the CA2 region. Future research which could be undertaken could focus on a few of the established properties of the CA2, or on the techniques of modelling behaviour. As well as the behavioural tests which were already undertaken by the supervisor (unpublished data), techniques for modelling behaviour in rodents could be used on *Rest* cKO mice to narrow the conclusions already made on the behavioural phenotype. There has been an innumerable quantity of behavioural assays presented which evaluate compulsive like behaviours, for example, the marble burying test and the nestlet shredding test being those with the greatest validity (Witkin, 2008; Angoa-Perez *et al.*, 2013). Both assays taking advantage of the natural proclivity and the spontaneous behaviour of the rodents. Though, modelling behaviour in rodents, particularly compulsive related behaviours proves great difficulty.

When analysing the findings using synaptophysin, it was apparent that the staining seemed to have worked, although it was hard to visualise the synapses and evaluate. Comparing this to the research by Saura *et al.*, (2004) raises questions about the neurodegenerative phenotype. The previous study suggests a very clear difference in staining of synapses between the two genotypes studied. Due to this, when comparing the findings from the previous study and that of the present study, it can be concluded that there is no neurodegenerative phenotype seen in *Rest* cKO when analysing a marker of synaptic terminals.

7.0 Concluding remarks

This study used a REST conditional knockout model not previously used for these purposes, to explore the molecular mechanisms and biochemical processes which play a role in REST regulation. This was undertaken to try and understand changes at the protein level and possible neurodegenerative phenotypes. A few of the findings obtained were as hypothesised and replicate results seen by previous studies. However, other interesting findings attained need further validation to be able to fully comprehend their meaning.

This study was able to conclude that control samples have stronger levels of the phosphorylated CREB protein when compared to the *Rest* cKO genotype, which could possibly, if reproduced explain the memory phenotype as well as explain the role of REST regulation with regards to AD. Similarly, this study also establishes motivating findings when analysing protein levels of vasopressin V1B receptor and observing phenotypes in the CA2 region relating to social memory.

Using an *in vivo* experimental system, this study has enabled further research to be undertaken on the role of REST which has contributed to a greater understanding of the regulation of REST dependant proteins. Though there is a need for replication of results, it may constitute a step further in considering new possibilities for therapeutic interventions in AD or conditions related to social memory.

8.0 References

- Abner, E., Jicha, G., Shaw, L., Trojanowski, J. and Goetzl, E. (2016). Plasma neuronal exosomal levels of Alzheimer's disease biomarkers in normal aging. *Annals of Clinical and Translational Neurology*, 3(5), 399-403.
- Alexander, G., Farris, S., Pirone, J., Zheng, C., Colgin, L. and Dudek, S. (2016). Social and novel contexts modify hippocampal CA2 representations of space. *Nature Communications*, 7(1).
- Angoa-Perez, M., Kane, M. J., Briggs, D. I., Francescutti, D. M. and Kuhn, D. M. (2013). Marble burying and nestlet shredding as tests of repetitive, compulsive-like behaviors in mice. *Journal of visualized experiments*, 82, 50978.
- Ashton, N., Hye, A., Leckey, C., Jones, A., Gardner, A., Elliott, C., Wetherell, J., Lenze, E., Killick, R. and Marchant, N. (2017). Plasma REST: a novel candidate biomarker of Alzheimer's disease is modified by psychological intervention in an at-risk population. *Translational Psychiatry*, 7(6).
- Ballas, N., Battaglioli, E., Atouf, F., Andres, M., Chenoweth, J., Anderson, M., Burger, C., Moniwa, M., Davie, J., Bowers, W., Federoff, H., Rose, D., Rosenfeld, M., Brehm, P. and Mandel, G. (2001). Regulation of Neuronal Traits by a Novel Transcriptional Complex. *Neuron*, 31(3).
- Bartolotti, N., Bennett, D. A. and Lazarov, O. (2016). Reduced pCREB in Alzheimer's disease prefrontal cortex is reflected in peripheral blood mononuclear cells. *Molecular Psychiatry*, 21(9), 1158–1166.
- Behan, D., Heinrichs, S., Troncoso, J., Liu, X., Kawas, C., Ling, N. and De Souza, E. (1995). Displacement of corticotropin releasing factor from its binding protein as a possible treatment for Alzheimer's disease. *Nature*, 378(6554), 284-287.
- Benoy, A., Dasgupta, A. and Sajikumar, S. (2018). Hippocampal area CA2: an emerging modulatory gateway in the hippocampal circuit. *Experimental Brain Research*, 236(4), 919-931.
- Bersten, D., Bruning, J., Peet, D. and Whitelaw, M. (2014). Human Variants in the Neuronal Basic Helix-Loop-Helix/Per-Arnt-Sim (bHLH/PAS) Transcription Factor Complex NPAS4/ARNT2 Disrupt Function. *PLoS ONE*, 9(1), 85768.
- Bozon, B., Davis, S. and Laroche, S. (2002). Regulated transcription of the immediate-early gene Zif268: Mechanisms and gene dosage-dependent function in synaptic plasticity and memory formation. *Hippocampus*, 12(5), 570-577.
- Calais, J., Valvassori, S., Resende, W., Feier, G., Athié, M., Ribeiro, S., Gattaz, W., Quevedo, J. and Ojopi, E. (2013). Long-term decrease in immediate early gene expression after electroconvulsive seizures. *Journal of Neural Transmission*, 120(2), 259-266.
- Carstens, K., Phillips, M., Pozzo-Miller, L., Weinberg, R. and Dudek, S. (2016). Perineuronal Nets Suppress Plasticity of Excitatory Synapses on CA2 Pyramidal Neurons. *The Journal of Neuroscience*, 36(23), 6312-6320.
- Chen, Z.F., Paquette, A.J. and Anderson, D.J. (1998). NRSF/REST is required *in vivo* for repression of multiple neuronal target genes during embryogenesis. *Nature Genetics*, (20), 136-42.

Chevalleyre, V. and Piskorowski, R. (2016). Hippocampal Area CA2: An Overlooked but Promising Therapeutic Target. *Trends in Molecular Medicine*, 22(8), 645-655.

Chin, J. (2005). Fyn Kinase Induces Synaptic and Cognitive Impairments in a Transgenic Mouse Model of Alzheimer's Disease. *Journal of Neuroscience*, 25(42), 9694-9703.

Corbett, B., You, J., Zhang, X., Pyfer, M., Tosi, U., Iascone, D., Petrof, I., Hazra, A., Fu, C., Stephens, G., Ashok, A., Aschmies, S., Zhao, L., Nestler, E. and Chin, J. (2017). Δ FosB Regulates Gene Expression and Cognitive Dysfunction in a Mouse Model of Alzheimer's Disease. *Cell Reports*, 20(2), 344-355.

DeVito, L., Konigsberg, R., Lykken, C., Sauvage, M., Young, W. and Eichenbaum, H. (2009). Vasopressin 1b Receptor Knock-Out Impairs Memory for Temporal Order. *Journal of Neuroscience*, 29(9), 2676-2683.

Dudek, S. M., Alexander, G. M. and Farris, S. (2016). Rediscovering area CA2: unique properties and functions. *Nature reviews. Neuroscience*, 17(2), 89-102.

Duran, J., Antonio, L., Pacheco-Otalora, L., Garrido-Sanabria, E. and Colom, L. (2013). Characterization of a transgenic model of Alzheimer's disease: The influence of Npas4 gene expression on the development of the pathology. *Alzheimer's & Dementia*, 9(4), 556.

Echeverria, V., Ducatenzeiler, A., Dowd, E., Jänne, J., Grant, S., Szyf, M., Wandosell, F., Avila, J., Grimm, H., Dunnett, S., Hartmann, T., Alhonen, L. and Cuervo, A. (2004). Altered mitogen-activated protein kinase signaling, tau hyperphosphorylation and mild spatial learning dysfunction in transgenic rats expressing the β -amyloid peptide intracellularly in hippocampal and cortical neurons. *Neuroscience*, 129(3), 583-592.

Espana, J., Valero, J., Minano-Molina, A., Masgrau, R., Martin, E., Guardia-Laguarta, C., Lleo, A., Gimenez-Llort, L., Rodriguez-Alvarez, J. and Saura, C. (2010). β -Amyloid Disrupts Activity-Dependent Gene Transcription Required for Memory through the CREB Coactivator CRTC1. *Journal of Neuroscience*, 30(28), 9402-9410.

Estus, S. (1994). Altered gene expression in neurons during programmed cell death: identification of c-jun as necessary for neuronal apoptosis. *The Journal of Cell Biology*, 127(6), 1717-1727.

Fleischmann, A., Hvalby, O., Jensen, V., Strekalova, T., Zacher, C., Layer, L., Kvello, A., Reschke, M., Spanagel, R., Sprengel, R., Wagner, E. and Gass, P. (2003). Impaired Long-Term Memory and NR2A-Type NMDA Receptor-Dependent Synaptic Plasticity in Mice Lacking c-Fos in the CNS. *The Journal of Neuroscience*, 23(27), 9116-9122.

Franklin, K. and Paxinos, G. (2019). *Paxino's and Franklin's the Mouse Brain in Stereotaxic Coordinates*. San Diego: Elsevier Science & Technology.

Gao, Z., Ure, K., Ding, P., Nashaat, M., Yuan, L., Ma, J., Hammer, R. and Hsieh, J. (2011). The Master Negative Regulator REST/NRSF Controls Adult Neurogenesis by Restraining the Neurogenic Program in Quiescent Stem Cells. *Journal of Neuroscience*, 31(26), 9772-9786.

Geula, C., Nagykerly, N., Nicholas, A. and Wu, C. (2008). Cholinergic Neuronal and Axonal Abnormalities Are Present Early in Aging and in Alzheimer Disease. *Journal of Neuropathology & Experimental Neurology*, 67(4), 309-318.

Gong, B., Vitolo, O. V., Trinchese, F., Liu, S., Shelanski, M. and Arancio, O. (2004). Persistent improvement in synaptic and cognitive functions in an Alzheimer mouse model after rolipram treatment. *The Journal of clinical investigation*, 114(11), 1624–1634.

González-Castañeda, R., Sánchez-González, V., Flores-Soto, M., Vázquez-Camacho, G., Macías-Islas, M. and Ortiz, G. (2013). Neural restrictive silencer factor and choline acetyltransferase expression in cerebral tissue of Alzheimer's Disease patients: a pilot study. *Genetics and Molecular Biology*, 36(1), 025-036.

Gonzalez-Lima, F. (1998). Cytochrome Oxidase in Neuronal Metabolism and Alzheimer's Disease: Proceedings of an International Symposium Held in New Orleans, Louisiana, October 28, 1997 (Aging). *The British Journal of Psychiatry*. Springer.

Guan, J., Haggarty, S., Giacometti, E., Dannenberg, J., Joseph, N., Gao, J., Nieland, T., Zhou, Y., Wang, X., Mazitschek, R., Bradner, J., DePinho, R., Jaenisch, R. and Tsai, L. (2009). HDAC2 negatively regulates memory formation and synaptic plasticity. *Nature*, 459(7243), 55-60.

Guzowski, J., Lyford, G., Stevenson, G., Houston, F., McGaugh, J., Worley, P. and Barnes, C. (2000). Inhibition of Activity-Dependent Arc Protein Expression in the Rat Hippocampus Impairs the Maintenance of Long-Term Potentiation and the Consolidation of Long-Term Memory. *The Journal of Neuroscience*, 20(11), 3993-4001.

Gyllys, K. H., Fein, J. A., Yang, F., Wiley, D. J., Miller, C. A. and Cole, G. M. (2004). Synaptic Changes in Alzheimer's Disease: Increased Amyloid- β and Gliosis in Surviving Terminals Is Accompanied by Decreased PSD-95 Fluorescence. *The American Journal of Pathology*, 165(5), 1809–1817.

He, J. (2002). A Role of Fos Expression in the CA3 Region of the Hippocampus in Spatial Memory Formation in Rats. *Neuropsychopharmacology*, 26(2), 259-268.

Heese, K. and Akatsu, H. (2006). Alzheimers Disease - An Interactive Perspective. *Current Alzheimer Research*, 3(2), 109-121.

Hitti, F. and Siegelbaum, S. (2014). The hippocampal CA2 region is essential for social memory. *Nature*, 508(7494), 88-92.

Horii-Hayashi, N., Sasagawa, T., Hashimoto, T., Kaneko, T., Takeuchi, K. and Nishi, M. (2015). A newly identified mouse hypothalamic area having bidirectional neural connections with the lateral septum: the perifornical area of the anterior hypothalamus rich in chondroitin sulfate proteoglycans. *European Journal of Neuroscience*, 42(6), 2322-2334.

Huber, G. and Matus, A. (1984). Differences in the cellular distributions of two microtubule-associated proteins, MAP1 and MAP2, in rat brain. *The Journal of Neuroscience*, 4(1), 151-160.

Hwang, J., Aromolaran, K. and Zukin, R. (2017). The emerging field of epigenetics in neurodegeneration and neuroprotection. *Nature Reviews Neuroscience*, 18(6), 347-361.

Hwang, J. and Zukin, R. (2018). REST, a master transcriptional regulator in neurodegenerative disease. *Current Opinion in Neurobiology*, 48, 193-200.

Kamarulzaman, N., Dewadas, H., Leow, C., Yaacob, N. and Mokhtar, N. (2017). The role of REST and HDAC2 in epigenetic dysregulation of Nav1.5 and nNav1.5 expression in breast cancer. *Cancer Cell International*, 17(1).

Kandel, E. R. (2012). The molecular biology of memory: cAMP, PKA, CRE, CREB-1, CREB-2, and CPEB. *Molecular Brain*, 5, 14.

Kandimalla, R., Manczak, M., Yin, X., Wang, R. and Reddy, P. (2017). Hippocampal phosphorylated tau induced cognitive decline, dendritic spine loss and mitochondrial abnormalities in a mouse model of Alzheimer's disease. *Human Molecular Genetics*, 27(1), 30-40.

Kasahara, M., Groenink, L., Kas, M., Bijlsma, E., Olivier, B. and Sarnyai, Z. (2011). Influence of transgenic corticotropin-releasing factor (CRF) over-expression on social recognition memory in mice. *Behavioural Brain Research*, 218(2), 357-362.

Kobayashi, E., Nakano, M., Kubota, K., Himuro, N., Mizoguchi, S., Chikenji, T., Otani, M., Mizue, Y., Nagaishi, K. and Fujimiya, M. (2018). Activated forms of astrocytes with higher GLT-1 expression are associated with cognitive normal subjects with Alzheimer pathology in human brain. *Scientific Reports*, 8(1).

Korosi, A., Shanabrough, M., McClelland, S., Liu, Z., Borok, E., Gao, X., Horvath, T. and Baram, T. (2010). Early-Life Experience Reduces Excitation to Stress-Responsive Hypothalamic Neurons and Reprograms the Expression of Corticotropin-Releasing Hormone. *Journal of Neuroscience*, 30(2), 703-713.

Lansdall, C. (2014). An effective treatment for Alzheimer's disease must consider both amyloid and tau. *Bioscience Horizons*, 7(0).

Lensjo, K., Lepperod, M., Dick, G., Hafting, T. and Fyhn, M. (2017). Removal of Perineuronal Nets Unlocks Juvenile Plasticity Through Network Mechanisms of Decreased Inhibition and Increased Gamma Activity. *The Journal of Neuroscience*, 37(5), 1269-1283.

Lin, Y., Bloodgood, B., Hauser, J., Lapan, A., Koon, A., Kim, T., Hu, L., Malik, A. and Greenberg, M. (2008). Activity-dependent regulation of inhibitory synapse development by Npas4. *Nature*, 455(7217), 1198-1204.

Lin, Y., Hsieh, T., Tsai, T., Chen, C., Huang, C. and Hsu, K. (2017). Conditional Deletion of Hippocampal CA2/CA3a Oxytocin Receptors Impairs the Persistence of Long-Term Social Recognition Memory in Mice. *The Journal of Neuroscience*, 38(5), 1218-1231.

Liu, W., Wang, C., Cui, Y., Mo, L., Zhi, J., Sun, S., Wang, Y., Yu, H., Zhao, C., Feng, J. and Chen, P. (2006). Inhibition of neuronal nitric oxide synthase antagonizes morphine antinociceptive tolerance by decreasing activation of p38 MAPK in the spinal microglia. *Neuroscience Letters*, 410(3), 174-177.

Lu, L., Igarashi, K., Witter, M., Moser, E. and Moser, M. (2015). Topography of Place Maps along the CA3-to-CA2 Axis of the Hippocampus. *Neuron*, 87(5), 1078-1092.

Lu, T., Aron, L., Zullo, J., Pan, Y., Kim, H., Chen, Y., Yang, T., Kim, H., Drake, D., Liu, X., Bennett, D., Colaiácovo, M. and Yankner, B. (2014). REST and stress resistance in ageing and Alzheimer's disease. *Nature*, 507(7493), 448-454.

Ma, Y., Chen, K., Wei, C. and Lee, E. (1999). Corticotropin-releasing factor enhances brain-derived neurotrophic factor gene expression to facilitate memory retention in rats. *Chinese Journal of Physiology*, 42(2), 73-81.

Mankin, E., Diehl, G., Sparks, F., Leutgeb, S. and Leutgeb, J. (2015). Hippocampal CA2 Activity Patterns Change over Time to a Larger Extent than between Spatial Contexts. *Neuron*, 85(1), 190-201.

Marchant, N., Ashton, N., Hye, A. and Lovestone, S. (2015). Investigation of REST protein in healthy elderly and Alzheimer's disease using a blood-based approach. *Alzheimer's & Dementia*, 11(7), 652.

Marcus, D., Strafaci, J., Miller, D., Masia, S., Thomas, C., Rosman, J., Hussain, S. and Freedman, M. (1998). Quantitative neuronal c-Fos and c-Jun expression in Alzheimer's disease. *Neurobiology of Aging*, 19(5), 393-400.

Minucci, S. and Pelicci, P. (2006). Histone deacetylase inhibitors and the promise of epigenetic (and more) treatments for cancer. *Nature Reviews Cancer*, 6(1), 38-51.

Mou, X. (2016). Hippocampal CA2 Region: A New Player in Social Dysfunctions. *Journal of Neurology & Neurophysiology*, 07(01).

Ochiishi, T., Saitoh, Y., Yukawa, A., Saji, M., Ren, Y., Shirao, T., Miyamoto, H., Nakata, H. and Sekino, Y. (1999). High level of adenosine A1 receptor-like immunoreactivity in the CA2/CA3a region of the adult rat hippocampus. *Neuroscience*, 93(3), 955-967.

Orta-Salazar, E., Aguilar-Vázquez, A., Martínez-Coria, H., Luquín-De Anda, S., Rivera-Cervantes, M., Beas-Zarate, C., Feria-Velasco, A. and Díaz-Cintra, S. (2014). REST/NRSF-induced changes of ChAT protein expression in the neocortex and hippocampus of the 3xTg-AD mouse model for Alzheimer's disease. *Life Sciences*, 116(2), 83-89.

Palop, J., Jones, B., Kekonius, L., Chin, J., Yu, G., Raber, J., Masliah, E. and Mucke, L. (2003). Neuronal depletion of calcium-dependent proteins in the dentate gyrus is tightly linked to Alzheimer's disease-related cognitive deficits. *Proceedings of the National Academy of Sciences*, 100(16), 9572-9577.

Palop, J. (2005). Vulnerability of Dentate Granule Cells to Disruption of Arc Expression in Human Amyloid Precursor Protein Transgenic Mice. *Journal of Neuroscience*, 25(42), 9686-9693.

Plath, N., Ohana, O., Dammermann, B., Errington, M., Schmitz, D., Gross, C., Mao, X., Engelsberg, A., Mahlke, C., Welzl, H., Kobalz, U., Stawrakakis, A., Fernandez, E., Waltereit, R., Bick-Sander, A., Therstappen, E., Cooke, S., Blanquet, V., Wurst, W., Salmen, B., Bösl, M., Lipp, H., Grant, S., Bliss, T., Wolfer, D. and Kuhl, D. (2006). Arc/Arg3.1 Is Essential for the Consolidation of Synaptic Plasticity and Memories. *Neuron*, 52(3), 437-444.

Poirel, O., Mella, S., Videau, C., Ramet, L., Davoli, M., Herzog, E., Katsel, P., Mechawar, N., Haroutunian, V., Epelbaum, J., Daumas, S. and El Mestikawy, S. (2018). Moderate decline in select

synaptic markers in the prefrontal cortex (BA9) of patients with Alzheimer's disease at various cognitive stages. *Scientific Reports*, 8(1).

Pugazhenthii, S., Wang, M., Pham, S., Sze, C.-I. and Eckman, C. B. (2011). Downregulation of CREB expression in Alzheimer's brain and in A β -treated rat hippocampal neurons. *Molecular Neurodegeneration*, 6, 60.

Qin, X., Wang, Y. and Paudel, H. (2017). Inhibition of Early Growth Response 1 in the Hippocampus Alleviates Neuropathology and Improves Cognition in an Alzheimer Model with Plaques and Tangles. *The American Journal of Pathology*, 187(8), 1828-1847.

Qiu, J., Dunbar, D., Noble, J., Cairns, C., Carter, R., Kelly, V., Chapman, K., Seckl, J. and Yau, J. (2016). Decreased Npas4 and Arc mRNA levels in the hippocampus of aged memory-impaired wild-type but not memory preserved 11 β -HSD1 deficient mice. *Journal of Neuroendocrinology*, 28(1).

Raam, T., McAvoy, K., Besnard, A., Veenema, A. and Sahay, A. (2017). Hippocampal oxytocin receptors are necessary for discrimination of social stimuli. *Nature Communications*, 8(1).

Ramamoorthi, K., Fropf, R., Belfort, G., Fitzmaurice, H., McKinney, R., Neve, R., Otto, T. and Lin, Y. (2011). Npas4 regulates a transcriptional program in CA3 required for contextual memory formation. *Science*, 334(6063), 1669-1675.

Renthal, W., Carle, T., Maze, I., Covington, H., Truong, H., Alibhai, I., Kumar, A., Montgomery, R., Olson, E. and Nestler, E. (2008). FosB Mediates Epigenetic Desensitization of the c-fos Gene After Chronic Amphetamine Exposure. *Journal of Neuroscience*, 28(29), 7344-7349.

Rodriguez-Arellano, J., Parpura, V., Zorec, R. and Verkhratsky, A. (2016). Astrocytes in physiological aging and Alzheimer's disease. *Neuroscience*, 323, 170-182.

Rudinskiy, N., Hawkes, J., Betensky, R., Eguchi, M., Yamaguchi, S., Spires-Jones, T. and Hyman, B. (2012). Orchestrated experience-driven Arc responses are disrupted in a mouse model of Alzheimer's disease. *Nature Neuroscience*, 15(10), 1422-1429.

Safieh, M., Korczyn, A.D. and Michaelson, D.M. (2019). ApoE4: an emerging therapeutic target for Alzheimer's disease. *BMC Medicine*, 17, 64.

Saura, C., Choi, S., Beglopoulos, V., Malkani, S., Zhang, D., Rao, B., Chattarji, S., Kelleher, R., Kandel, E., Duff, K., Kirkwood, A. and Shen, J. (2004). Loss of Presenilin Function Causes Impairments of Memory and Synaptic Plasticity Followed by Age-Dependent Neurodegeneration. *Neuron*, 42(1), 23-36.

Saura, C. and Valero, J. (2011). The role of CREB signaling in Alzheimer's disease and other cognitive disorders. *Reviews in the Neurosciences*, 22(2).

Scheff, S., Price, D., Schmitt, F., DeKosky, S. and Mufson, E. (2007). Synaptic alterations in CA1 in mild Alzheimer disease and mild cognitive impairment. *Neurology*, 68(18), 1501-1508.

Selkoe, D.J. (2002). Alzheimer's disease is a synaptic failure. *Science*, 298, 789-791.

Sheffield, M. and Dombeck, D. (2019). Dendritic mechanisms of hippocampal place field formation. *Current Opinion in Neurobiology*, 54, 1-11.

Smeyne, R., Vendrell, M., Hayward, M., Baker, S., Miao, G., Schilling, K., Robertson, L., Curran, T. and Morgan, J. (1993). Continuous c-fos expression precedes programmed cell death in vivo. *Nature*, 363(6425), 166-169.

Smith, A. S., Williams Avram, S. K., Cymerblit-Sabba, A., Song, J. and Young, W. S. (2016). Targeted activation of the hippocampal CA2 area strongly enhances social memory. *Molecular psychiatry*, 21(8), 1137-44.

Sofroniew, M. V. and Vinters, H. V. (2010). Astrocytes: biology and pathology. *Acta neuropathologica*, 119(1), 7-35.

Sorg, B., Berretta, S., Blacktop, J., Fawcett, J., Kitagawa, H., Kwok, J. and Miquel, M. (2016). Casting a Wide Net: Role of Perineuronal Nets in Neural Plasticity. *The Journal of Neuroscience*, 36(45), 11459-11468.

Stevenson, E. and Caldwell, H. (2014). Lesions to the CA2 region of the hippocampus impair social memory in mice. *European Journal of Neuroscience*, 40(9), 3294-3301.

Verge, G., Milligan, E., Maier, S., Watkins, L., Naeve, G. and Foster, A. (2004). Fractalkine (CX3CL1) and fractalkine receptor (CX3CR1) distribution in spinal cord and dorsal root ganglia under basal and neuropathic pain conditions. *European Journal of Neuroscience*, 20(5), 1150-1160.

Wersinger, S., Ginns, E., O'Carroll, A., Lolait, S. and Young III, W. (2002). Vasopressin V1b receptor knockout reduces aggressive behavior in male mice. *Molecular Psychiatry*, 7(9), 975-984.

Witkin, J. (2008). Animal Models of Obsessive-Compulsive Disorder. *Current Protocols in Neuroscience*.

Wolf, N., Zimmerman, M. and Johnson, G. (1999). Hippocampal microtubule-associated protein-2 alterations with contextual memory. *Brain Research*, 821(1), 241-249.

Wu, J. and Xie, X. (2006). Comparative sequence analysis reveals an intricate network among REST, CREB and miRNA in mediating neuronal gene expression. *Genome Biology*, 7, 85.

Wyss-Coray, T., Loike, J., Brionne, T., Lu, E., Anankov, R., Yan, F., Silverstein, S. and Husemann, J. (2003). Adult mouse astrocytes degrade amyloid- β in vitro and in situ. *Nature Medicine*, 9(4), 453-457.

Young, W., Li, J., Wersinger, S. and Palkovits, M. (2006). The vasopressin 1b receptor is prominent in the hippocampal area CA2 where it is unaffected by restraint stress or adrenalectomy. *Neuroscience*, 143(4), 1031-1039.

Zhang, J., Chen, L., Lv, Z., Niu, X., Shao, C., Zhang, C., Pruski, M., Huang, Y., Qi, C., Song, N., Lang, B. and Ding, Y. (2016). Oxytocin is implicated in social memory deficits induced by early sensory deprivation in mice. *Molecular Brain*, 9(1).

9.0 Appendix

Appendix A: Preparation of Reagents

Nissl substance:

Cresyl violet 0.5% solution

After preparation, filter solution.

Nuclear preparation buffer A:

10mM Tris, pH 7.5

100mM NaCl

1% Triton

0.1mM EDTA

0.5mM PMSF

Merck cOmplete, Mini, EDTA-free Protease Inhibitor Cocktail (1 tablet per 10ml)

RIPA buffer:

25mM Tris, pH 7.5

150mM NaCl

1% NP-40

1% Sodium deoxycholate

0.1% SDS

RIPA supplementary buffer:

75mM Tris, pH 7.5

150mM NaCl

10mM EDTA

1.9% SDS

Lysis buffer:

50mM Tris, pH 7.5

150mM NaCl

5mM EDTA

0.5% NP-40

0.5% Sodium deoxycholate

1% SDS

Merck cOmplete, Mini, EDTA-free Protease Inhibitor Cocktail (1 tablet per 10ml)

0.2M PB stock:

0.2M NaH₂PO₄ * H₂O

0.2M Na₂HPO₄

Mix the two solutions

PBS:

950ml dH₂O with 50ml of 0.2M PB stock

Add 9g of NaCl

PBS-Tween:

0.5ml of Tween-20 in 1 litre of PBS

